Connection details between Composite Beam and Cross-Laminated Timber slab

HÄMEEN AMMATTIKORKEAKOULU
HÄME UNIVERSITY OF APPLIED SCIENCES

Bachelor's thesis

Hämeenlinna University Center, Degree Programme in Construction Engineering

Spring 2020

Pavel Zhukov

HÄMEEN AMMATTIKORKEAKOULU
HÄME UNIVERSITY OF APPLIED SCIENCES

Degree programme in Construction Engineering
Hämeenlinna University Centre

Author Pavel Zhukov **Year** 2020

Subject Connection details between Composite Beam and Cross-Laminated Timber Slab

Supervisors Cristina Tirteu, Jaakko Yrjölä, Juuso Salonen

ABSTRACT

The aim of the Bachelor's thesis was to describe and evaluate the most common connection details between steel-concrete composite (SCC) beam DELTABEAM® and Cross-Laminated Timber (CLT) slab in two variations: with and without concrete topping. The purpose of the thesis was to provide a basis for future studies that are to expand the CLT range of appliance in Finland.

The thesis was based on a theoretical description of the four different connectors that utilize the same working principles as the connections used for joining concrete floor slabs and the beam using the German standard details. The calculations were done according to the Eurocode 1995 and German timber design code DIN1052.

The result of the thesis was the connection details library. The result of the study allows to conclude that by using described connection details, the CLT slabs and DELTABEAM® form a reliable flooring system.

Keywords Composite beam, CLT, timber slab, connection details

Pages 61 pages including appendices 35 pages

CONTENTS

1 INTRODUCTION

Composite floor systems comprising steel concrete composite (SCC) beam DELTABEAM® and CLT slabs have already found applications in various type of buildings in Germany and Austria. The number of buildings utilizing such composite systems is constantly increasing all over the world. High load-carrying capacity, and aesthetics of the wooden composite structures makes it a promising addition to building traditions in many European countries.

1.1 Background

The performance of timber composite floor systems directly depends on the reliability of the connection details joining the structural elements. The purpose of the connectors is to ensure the save transfer of loads throughout its entire life cycle.
These demands are well met by the joints used in DELTABEAM®-concrete slab flooring systems. The connections and load transfer mechanism are well-studied and test proven, which provides a solid base for connection details between CLT and DELTABEAM® investigation.

1.2 Objectives

The thesis is limited to calculations of the case studies with three parallel beams supporting CLT slab and DELTABEAM®, and as a result, to obtain the connection detail library. The evaluation is done by design analysis with reference to connections used for joining concrete slabs with SCC beams and the German standard details. The calculations are based on the following design standards: Eurocodes 1993-1-1, 1995-1-1,2; and German timber design code DIN1052.

1.3 Scope and limitations

The thesis is limited to calculations of the case studies with three parallel beams supporting CLT slabs. Two low frequency (9 Hz<) one way spanning slabs with and without concrete topping are discussed. Beam supports are considered to be ultimately rigid. Ambient conditions, namely temperature (20 °C) and relative humidity (RH<65%), are assumed to be constant with time; hence, timber property and geometry change caused by shrinkage or creep of wood is neglected.

2 SLIM-FLOOR COMPOSITE SYSTEM

A composite is an element or a system of elements, consisting of one or more materials with different physical properties, bonded together and acting as a solid member. This provides more effective load distribution between the best mechanical properties of each material, that if they acted separately. Good example is (SCC) DELTABEAM®. The beam has high load carrying capacity which allows it to reach span length of 16 meters without large number of columns, which provides more open space (DELTABEAM® Slim Floor Structure Technical manual, 2014). Besides, slab positioning on ledges allows to save vertical space making the floor quite thin (Figure 1. a), in contrast with solutions where slabs are resting on beam top flange (Figure 1. b, c).

Figure 1. DELTABEAM(a), I-beam(b), Concrete beam(c).

The composite slim floor system consists of a floor slab, SCC beam DELTABEAM® and connection details between the steel-concrete section and the floor itself.

2.1 **CLT floor slab**

2.1.1 Technical specifications

Cross-Laminated Timber is one of massive timber products representatives. CLT is a planar timber product that is typically composed from an uneven number of mutually orthogonal lamination layers. Wood-based lamination panels are finger-jointed and glued together (Figure 2).

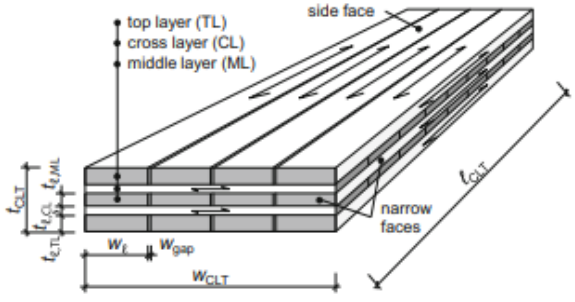

Figure 2. CLT floor slab.

Strength and stiffness of wooden decks depend on direction load is applied: parallel or perpendicular to the grain. Timber has the highest strength when the load is acting parallelly with the wood fibres direction. Consequently, in order to effectively accommodate forces derived due bending, typical pattern for one-way spanning floor slabs is formed of

parallel to the grain decks along the span in the bottom, and each subsequent odd layer. Such pattern allows to efficiently withstand bending and shear stresses.

In general, CLT slabs are made of softwood like pine or spruce of strength class C24 with moisture content of 12% +/- 2%. The characteristic properties of C24 are the following (Table 1).

Table 1. C24 timber characteristic properties.

	Strength Properties (in N/mm^2)					
	Bending	Tension Paralel	Tension Perpendicular	Compression Parallel	Compression Perpendicular	Shear
	$f_{m,k}$	$f_{t,0,k}$	$f_{t,90,k}$	$f_{c,0,k}$	$f_{c,90,k}$	$f_{v,k}$
C24	24	14	0.4	21	2.5	4

Stiffness properties (in kN/mm^2)				Density (in kg/m^3)	Density (in kg/m^3)
Mean modulus of elasticity parallel	5% modulus of elasticity parallel	Mean modulus of elasticity perpendicular	Mean shear modulus		
$E_{0,mean}$	$E_{0,05}$	$E_{90,mean}$	G_{mean}	ρ_k	ρ_{mean}
11	7.4	0.37	0.69	350	420

Sizes of boards that form lamination decks can have the height of 40 mm (in some cases it may reach 60 mm) and width of 300 mm. Currently the maximum production width (W_{CLT}) of a single CLT floor slab is 2.95 meters and span length (L_{CLT}) can reach 16 meters (Stora Enso CLT Technical brochure, 2017).

2.1.2 Slab types

There are two main slab configurations of CLT floor slabs, which are:

- **Basic**

CLT slab without any special covering except insulation or/and fire protective cladding (Figure 3).

Such a slab is quite light weight, which simplifies the erection process. However, rather thick slabs may be required for meeting the vibration requirements; thus, such slabs are usually short spanned.

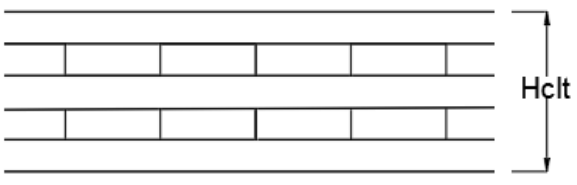

Figure 3. Basic CLT floor slab.

- **Composite slab**

A concrete cover layer is applied to the top surface of the CLT composite slab (Figure 4). The topping concrete is fastened to the CLT main face by means of the shear connection (screws, nails, notched connections etc.).

Timber-concrete composite slab has higher stiffness, consequently, the depth is decreased and longer spans can be released.

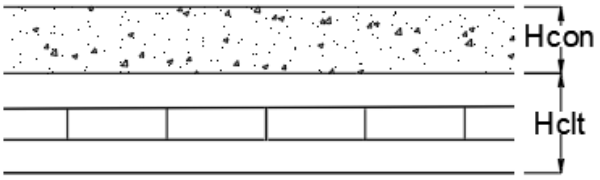

Figure 4. Composite CLT slab.

2.2 **Slim-floor composite beam**

2.2.1 Technical specifications

DELTABEAM® is a composite beam that consists of two basic components: welded steel section and concrete infill, which is poured through the casting holes (Figure 5) (DELTABEAM® Slim Floor Structure Technical manual, 2014).

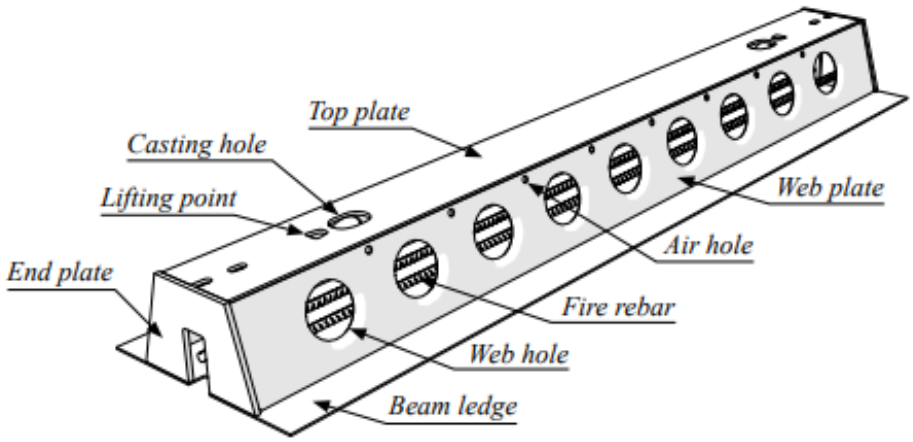

Figure 5. DELTABEAM® components.

Mechanical behaviour of the beam under applied loads depends on process stage it is one. These stages are the following:

- **Erection stage:** concrete infill hasn't reached its designed strength; hence the weight of the floor slab and accompanying construction loads are carried and transferred by the beam ledges.

- **Final (composite) stage:** when concrete infill has gained its designed strength, the beam acts as a composite member. Ledges at final stage are usually assumed to not function, thus all loads are directly transmitted to the webs through the shear interface (Leskelä, 1998, p.12).

2.2.2 Beam types

There are two basic types of DELTABEAM®s:

- **D-type:** the given beam is usually used as an intermediate floor carrying element due to ledge presence on both sides (Figure 6).

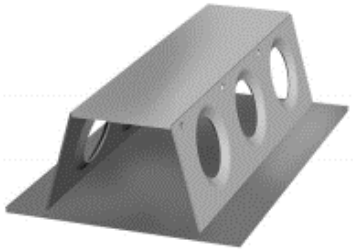

Figure 6. D-type DELTABEAM®**.**

- **DR-type:** this type of beam is used as an edge beam. The loads are transferred to the only one web (Figure 7).

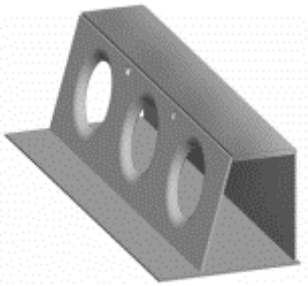

Figure 7. DR-type DELTABEAM®.

2.3 **Connection details**

There are two basic connection types with separate purposes: joint and torsion reinforcement.

2.3.1 Joint reinforcement

When the slab is subjected to bending the laterally restrained ends push against the DELTABEAM®'s inclined web, forming a compression arch through which the applied loads are transferred to the beam webs

(DELTABEAM® Slim Floor Structure Technical manual, 2014). Effectiveness of the compressive arch is dependent upon the longitudinal shear interface between the slab and the web surfaces. Joint reinforcement ensures proper shear interface between the slab side face and the beam inclined webs by tying the floor slab and the beam together (Leskelä, 1998, p.6). This interaction can be interrupted by beam's lateral displacement, concrete infill or slab geometry change caused by shrinkage. The minimum amount needed for preventing horizontal separation because shrinkage of the grouting, is 92 mm^2/m (Figure 8).

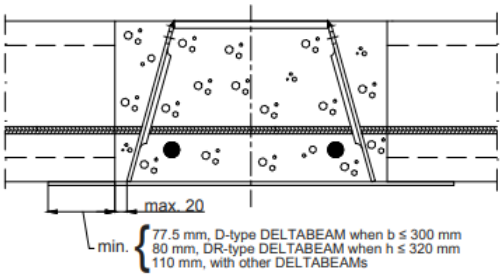

Figure 8. Joint reinforcement.

Practically the joint reinforcement positioning doesn't have an impact on the connection performance and is only restricted by additional or main web holes location. However, typically the reinforcement is placed in the compressed zone (below beam's neutral axis).

In accidental situations the slab is carried by dowel action of the joint reinforcement. Dowel action is activated when embedment failure occurs, and as a result the beam and the slab surfaces start to move along each other; afterwards, the reinforcement undergoes plastic deformation, and restricts further vertical displacement of the floor slab by, again, tying them together (Figure 9).

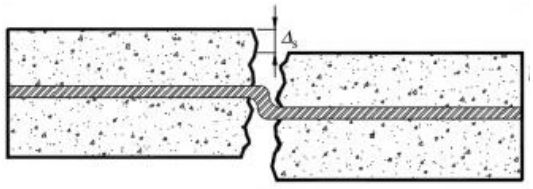

Figure 9. Dowel action.

2.3.2 Torsion reinforcement

When DELTABEAM® is subjected to torque moment caused by significant load difference, the risk of slabs to slip off rises; hence, torsion should be eliminated by applying a certain form of rotation preventing connection details. The functioning principle of D- and DR- beam types subjected to torsion is the following:

D-beams: When the beam us subjected to torsional moment and it tends to rotate around its axis, this movement is restrained by the slab (compression $\overrightarrow{C1}$; $\overrightarrow{C2}$) and the reinforcement (tension $\overrightarrow{T1}$; $\overrightarrow{T2}$). If the slabs and the grouting can handle the compressive forces $\overrightarrow{C1}$ and $\overrightarrow{C2}$ without failure or excessive deformation, torsion reinforcement may not be required (Figure 10).

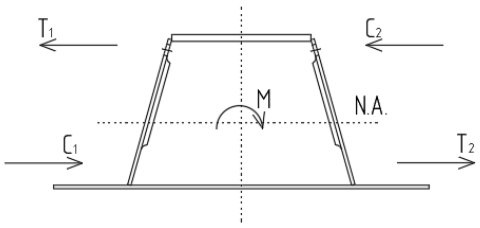

Figure 10. D-beams torsion schema.

DR-beams: In DR-Beams torsion is eliminated by slab in compression ($\vec{C}$) and the torsion reinforcement that ties the bottom of the beam and the slab together ($\vec{T}$) (Figure 11).

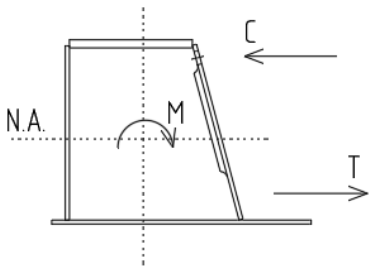

Figure 11. DR-beams torsion schema.

Regardless of the beam type, the effectiveness of torsion reinforcement the higher, the farther it is located for the beam's rotation point (Eq.1).

$$M = T_{1,2} \cdot e_{tor}\ [kN \cdot m] \quad \text{(Eq. 1)}$$

$T_{1,2}$– tension force vector [kN]
e_{tor}– lever arm; distance between the point of rotation and the force vector [mm]

3 CONNECTION DETAILS BETWEEN CLT SLAB AND DELTABEAM

The general principles of connection detailing between the timber floor and the DELTABEAM® remain unchanged. Connection details are hybrids of typical connection details for timber and concrete joined together by couplers or welds. For timber these connections are glued-in rods (GIR)

and screws; basic connectors for concrete, are headed studs, bent or straight ribbed reinforcing bars.

3.1 **General assumptions and procedures**

3.1.1 Loads acting on connections

There are two scenarios for load distribution on the connections. The first implies the absence of a gap between the slab and the beam (Figure 12):

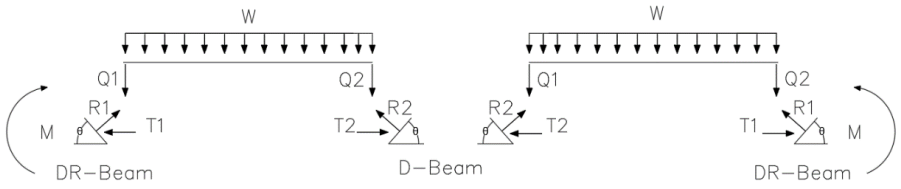

Figure 12. Loading diagram I.

The second takes into consideration the vertical displacement caused by gap appearance (Figure 13):

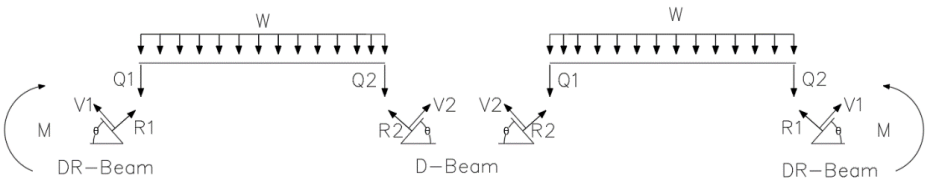

Figure 13. Loading diagram II.

Where:

W −line load acting on slab [kN/m]

$Q_1\ and\ Q_2$ −slab reaction forces [kN]

$R_1\ and\ R_2$ −ccompressive forces[kN]

$T_1\ and\ T_2$ −tensile forces[kN]

M −torque moment [kN/m]

The slabs are simply supported by the beams, so free rotation of the slab ends is not restricted, so the connections are basically subjected to tensile and shear forces only.

3.1.2 Connection slip modulus

Slip modulus of connection or also known as connection stiffness accounts the elastic or plastic deformation of the connected members. Deformation is defined as relative deformation of the centres of the fasteners in the original members (Jockwer & Steiger, 2016). Slip modulus of basic timber connections (dowels, screws) is determined as follows (Eq. 2,3):

$$K_{ser} = \frac{\rho_m{}^{1.5} \cdot d}{23} \; [N/mm] \text{(Eq.2)}$$

Where:

$$\rho_m = \sqrt{\rho_1 \cdot \rho_2} \; [kg/m^3] \text{ (Eq.3)}$$

d −diameter of the fastener (dowel, screw) [mm]
ρ_m −mean density of the connector [kg/m³]
$\rho_{1,2}$ −mean density of material 1 and 2 [kg/m³]

Slip modulus of the timber-concrete as well as steel-concrete, connections can be obtained based on the models given for the timber connection multiplied by a factor 2. The given approach is based on assumption that deformation of concrete and steel is negligibly small, and the connection stiffness then can be assumed to double of that from timber connections (Eurocode 1995-1-1).

The instantaneous deformation under service loads can be estimated as 40% of the connection load-carrying capacity (F_{Rd}) as per formula (Eq.4)

$$u_{inst} = \frac{0.4 \cdot F_{Rd}}{K_{ser}} \; [mm] \text{ (Eq.4)}$$

Since the stiffness of the connection is inversely proportional to the load, the slip can exceed the design limit in ultimate limit state. This can be accounted for by applying the general assumption that the slip modulus for ultimate limit state conditions is taken as 60-70% of the one at service state (Eq. 5):

$$K_u = \frac{2}{3} \cdot K_{ser} [N/mm] \text{ (Eq.5)}$$

Then, in order to define instantaneous slip of the connection at ULS the formula is applied (Eq. 6):

$$u_{inst} = \frac{0.4 \cdot F_{Rd}}{K_u} \; [mm] \text{ (Eq.6)}$$

3.1.3 Ledge deflection

As it was stated before, the slab loads at composite stage are transferred to the beam through the inclined webs, that is why the beam ledges are

usually assumed to be not acting. However, the ledge can be activated due to the slab's vertical movement caused by connection slip. The movement of the slab is described by vertical (*VS*) and horizontal (*HS*) slip magnitudes (Figure 14). The following schema is made for clarity if ledge activation and doesn't reflect the real deflection of the ledge. Dashed line represents the original position of the slab before slip, while solid line performs position of the slab after slip has taken place.

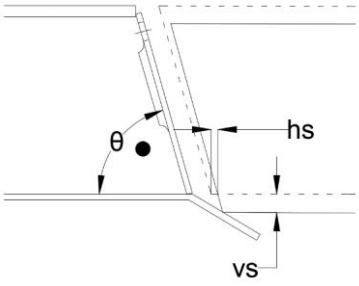

Figure 14. Ledge activation schema.

The movement will proceed till the slab meets another sustainable position on the web surface. This movement obeys the formula (Eq. 7):

$$vs = \frac{hs}{cot\ \theta}\ [mm] \text{ (Eq.7)}$$

The slip may lead to either inappropriate deflection or even failure of the ledge. These aspects should be considered in limit state design.

Deflection of the beam ledge is described by the formula (Eq. 8):

$$\delta_{ledge} = \frac{R\cdot\left(l_{ledge}+3\cdot s\right)^2\cdot\left(8\cdot l_{ledge}-3\cdot s\right)}{162\cdot E_{steel}\cdot I_{ledge}}\ [mm] \text{ (Eq.8)}$$

Where:

R −reaction force of the slab [kN]
l_{ledge} −length of the beam ledge [mm]
I_{ledge} −ledge second moment of area [mm^4]
E_{steel} −elastic modulus of steel [N/mm^2]
s −distance between the web and the slab [mm]

While bending stress in the ledge is calculated as follows (Eq.9):

$$\sigma = \frac{R\cdot l_{ledge}\cdot t_{ledge}}{6\cdot I_{ledge}}\ [N/mm^2] \text{ (Eq.9)}$$

Where:

t_{ledge} −ledge thickness [mm]

3.1.4 Shape of the slab

The floor slabs can have an inclined or straight narrow face shape. The shape of the slab affects the load distribution in connectors. Inclined shape is advisable as it enhances shear interaction between the slab and the beam, also limiting the vertical displacement.

Inclination de degree of the slab's narrow face is equal to the beam web's slant degree (approx. 74 degrees). The distance between the web and the slab (s) should be kept at a range of 40 mm (2 x max aggregate size + 5 [mm]; Eurocode 1992-1-1), in order to provide proper grouting and not to overload the beam ledge at erection stage and service limit state (Figure 15).

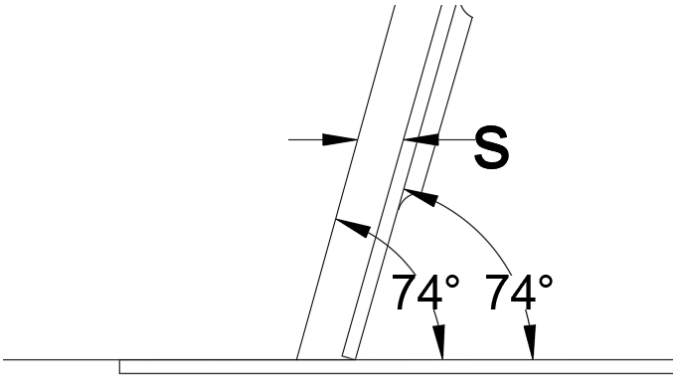

Figure 15. Slab slant degree.

3.2 **Limit state verification**

3.2.1 Timber

Timber as structural material has an indefinite nature and is rather susceptible to variable environmental conditions; as a result it suffers from changes in geometry and gradual weakening of the mechanical properties. Therefore, the characteristic properties of wood for design purposes must be reduced.

Design strengths of materials for ultimate limit state are obtained based on Eurocode 1995-1-1. The design strength of timber can be computed by means of the following formula (Eq.10):

$$R_d = k_{mod} \cdot \frac{R_k}{\gamma_M} \; [N/mm^2] \quad \text{(Eq.10)}$$

Where:

R_k *−characteristic strength value [N/mm²]*
γ_M *−partial safety factor [-]*

k_{mod} *−modification factor [-]*

Modification factor k_{mod} considers effect of ambient conditions and load duration. Recommended values for CLT used in buildings with consequence class CC1 of CC2 are shown in Table 2.

Table 2. Modification factors.

k_{mod}	Load duration
0.6	Permanent (>10 years)
0.7	Long (6 month – 10 years)
0.8	Medium (1 week-6 months)
0.9	Short (<1 week)
1.1	Very short (instantaneous)

3.2.2 Concrete

Infill concrete used in DELTABEAM® ranges from C20/25 to C30/37 depending on loads applied to the structure. C20/25 will be used in the further design procedures.

Mean compressive strength (Eq.11):

$$f_{cm} = f_{ck} + 8\ [N/mm^2] \text{ (Eq.11)}$$

Secant modulus of elasticity (Eq.12):

$$E_{cm} = 22000 \cdot \left(\frac{f_{cm}}{10}\right)^{0.3}\ [N/mm^2] \text{ (Eq.12)}$$

Design value of compressive strength (Eq.13):

$$R_d = \alpha_{cc} \cdot \frac{R_k}{\gamma_{M.c}} [N/mm^2]\ \text{(Eq.13)}$$

Where:

α_{cc} −reduction factor for concrete (EN1992-1-1 2.4.2.4) [-]
$\gamma_{M.s}$ − partial safety factor for concrete [-]

3.2.3 Steel

Design values for steel strength can be derived using the following equation (Eq.14):

$$R_d = \frac{R_k}{\gamma_{M.s}}\ [N/mm^2] \text{ (Eq.14)}$$

Where:
$\gamma_{M.s}$ − partial safety factor for steel [-]

3.3 **Fire design**

Wood is combustible material; thus, it is susceptive to fire, characteristic that works not in timbers favour when it comes to buildings with consequence class higher than CC1. In fact, the statement is only partly true for massive timber elements, which have stronger and thicker profiles that undergo fire exposure longer than usual light-weight wooden structural elements.

When a timber element exposed to fire reaches temperature of 100℃, water contained in wood starts to evaporate. At a temperature of 200-300℃ a process of thermal degradation (pyrolysis) takes place producing flammable gases, accompanied by a loss in mass. Fire design implies that the building doesn't collapse during a certain period of time stated by fire class. The collapse may occur due to inappropriate geometry loss, which leads to connection failure (Stora Enso, Fire protection, 2016, p.3).

Fire resistance requirements are fulfilled when joints are properly protected during fire exposure. Performance of CLT slabs in fire is similar to LVL or GLULAM, thus design procedures stated in Eurocode 1995-1-2 are relevant. The design is based on reduced load method (Eq. 15-18):

$$t_{d,fi} = -\frac{1}{k} \cdot \ln\left(\eta_{fi} \cdot \eta_0 \cdot \frac{k_{mod}}{\gamma_M} \cdot \frac{\gamma_{M,fi}}{k_{fi}}\right) \ [min] \quad \text{(Eq.15)}$$

Where:

$t_{d,fi}$ *−design fire resistance [min]*
η_{fi} *−reduction factor for the design load in the fire situation [-]*

$$\eta_{fi} = \frac{E_{d,fi}}{E_d}[-] \quad \text{(Eq.16)}$$

η_0 *−utiliziation degree at normal temperature [-]*

$$\eta_{fi} = \frac{F_{Ed}}{F_{Rd}}\ [-] \quad \text{(Eq.17)}$$

k_{mod} *−modification factor [-]*
$\gamma_{M,fi}$ *− partial safety factor for timber in fire [-]*
k_{fi} *− conversion coefficient for CLT [-]*
γ_M *−partial safety factor at normal temperature [-]*
k *−parameter factor (Eurocode 1994-1-2 Table 6.3) [-]*

Then the design value and required fire resistance time are compared.

$$\frac{h}{\beta_0} + t_{d,fi} > t_{req} \quad \text{(Eq.18)}$$

t_{req} *– required fire resistance time (60 min)*
β_0 *–charring rate [mm/min]*
h *–thickness of wood surrounding the connector*

3.3.1 Fire resistance improvement

Fire resistance is represented as time during which the given structure doesn't collapse (Eq.15). If the design fire resistance doesn't meet the fire class requirements, then the connector must be fireproofed by applying additional cladding as gypsum or wooden boards for example. Fire resistance increase is estimated by means of the following expressions (Eq.19-21):

$$t_{ch} = t_{ch.1} + t_{ch.2}\ [min] \text{ (Eq.19)}$$

Where:

$$t_{ch.1} = \frac{h_p}{\beta_0}\ [min] \text{ (Eq.20)}$$

h_p *–additional wooden board thickness [mm]*

$$t_{ch.2} = 2.8 \cdot (h_{gypsum}) - 14\ [min] \text{ (Eq.21)}$$

h_{gypsum} *– additional gypsum board thickness [mm]*

4 GLUED-IN DISCRETE THREADED RODS

4.1 **Description**

Glued-in Discrete Threaded Rod (GIDTR) is a form of prefabricated connections, which has high load carrying capacity and stiffness. Besides, theoretically, high fire resistance can be achieved due to the fact that the rod is surrounded by timber. However, high sensitivity of glues to elevated temperature must be considered (out of scope of the thesis).

GIDTR consists of two main components: glued-in and embedded in concrete segments. Both segments are interconnected by MODIX® coupler. One part of a steel threaded-rod is glued in a pre-drilled (parallel or perpendicular to the grain) hole at a narrow face of the CLT section by means of adhesive resin, while the second part of the rod with headed stud or bent end is embedded in the beam's concrete infill through a main or additional web hole (Figure 16).

The connector can be used as torsion as joint reinforcement.

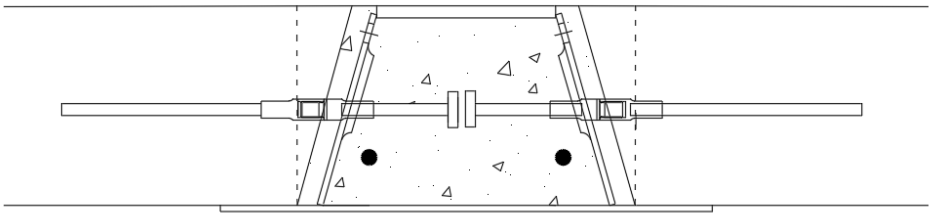

Figure 16. Glued-in Discrete Threaded rods.

4.1.1 Coupler

MODIX® Rebar Couplers are designed to provide slip-free bolted connections between reinforcement bars with a tensile/compressive resistance corresponding to the resistance of the connected reinforcement bar (Figure 17). The couplers can be seen in the same way as unspliced continuous reinforcement bars (MODIX® technical manual, 2016).

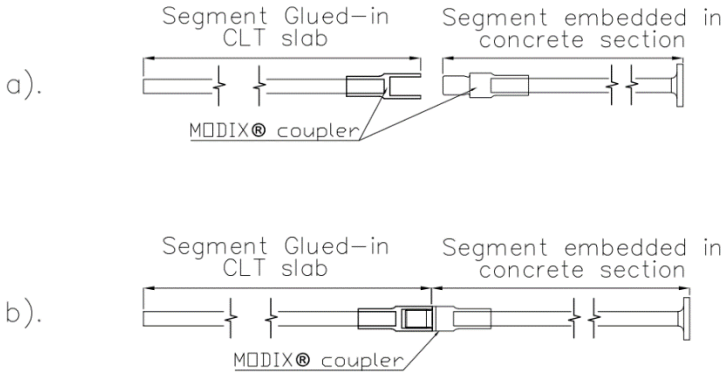

Figure 17. MODIX® coupler.

The basic coupler types used in the thesis are the following (Table 3):

Table 3. MODIX® standard couplers.

Coupler type*	SM10	SM12	SM14	SM16	SM20	SM25	SM28	SM32	SM40
Bar diameter [mm]	10	12	14	16	20	25	28	32	40

4.1.2 Glued-in segment

Glued-in segment refers to GIR connections, which are widely used in timber construction. Properly designed GIRs provide stiffness and high load-bearing capacity for the connection. Also, high durability and fire resistance can be released, due to the rod segment being surrounded by

wood. GIR connection consist of three components: timber, steel threaded rod and adhesive used to connect steel and timber. Mechanical properties of each component highly affect the connector performance (Tlustochowicz, 2011, p. 17).

- ***Timber properties***

Wood is orthotropic material and its mechanical properties are dependent upon the angle of the applied load, in relation to the grain direction (Green et al. 1999). The behaviour of timber is generally characterized as brittle when loaded in tension or shear (Gonzalez et al., 2016).

- ***Steel rod properties***

Favourable behaviour under ultimate loading in tension is ductile. Hot-rolled ribbed bars with characteristic yield strength of f_{yk} = 450 – 550 MPa can be used (MODIX® Rebar Coupler technical manual, 2016).

- ***Adhesive***

The following adhesive types are commonly used in GIR connections: phenol-resorcinol (PRF), epoxy (EPX) and polyurethane (PUR). Bengtsson and Johansson (2002) basing on test results concluded that among listed EPX has the highest pull-out strength, providing strong adhesion between steel and timber, consequently making timber the weakest part of the connection. According to Stepinac et al. (2013), PUR and EPX are the most used adhesives in Europe; therefore these adhesives will be used in design.

4.2 **Design process**

4.2.1 Shear resistance

Shear capacity of a rod in Ultimate Limit State (ULS) design is based on examining of the three possible failure modes. In accordance with Johansen yield theory (He et.al., 2016) these failure modes are the following:

1. Failure mode with rotation

In this failure mode the ultimate load-carrying capacity is achieved when the wood fails in a plastic manner along the fastener. It can be obtained by means of the following expressions (Eq.22-26) (Figure 18):

$$R_1 = \frac{f_{h,t,0} \cdot d_{rod} \cdot l_{CLT}}{1+\beta} \cdot \left(\sqrt{\beta + 2 \cdot \beta^2 \cdot \left(1 + \frac{l_{concrete}}{l_{CLT}} + \left(\frac{l_{concrete}}{l_{CLT}}\right)^2\right) + \beta^3 \cdot \left(\left(\frac{l_{concrete}}{l_{CLT}}\right)^2\right)} - \beta \cdot \left(1 + \frac{l_{concrete}}{l_{CLT}}\right) \right) [kN] \quad \text{(Eq.22)}$$

Embedment strength ratio:

$$\beta = \frac{f_{h,c}}{f_{h,t,0.90}} [-] \text{ (Eq.23)}$$

Concrete embedment strength:

$$f_{h,c} = \frac{P_u}{d_{rod} \cdot l_{concrete}} \ [N/mm^2] \text{ (Eq.24)}$$

$$P_u = 0.29 \cdot {d_{rod}}^2 \cdot \sqrt{f_{ck} \cdot E_{cm}} \ [kN] \text{ (Eq.25)}$$

Timber embedment strength:

$$f_{h,t,0} = 0.0435 \cdot (1 - 0.017 \cdot d_{rod}) \cdot {\rho_{CLT}}^{0.91} \ [N/mm^2] \text{ (Eq.26)}$$

d_{rod} *−diameter of the rod [mm]*
ρ_{CLT} *−density of CLT (350kg/m³)*

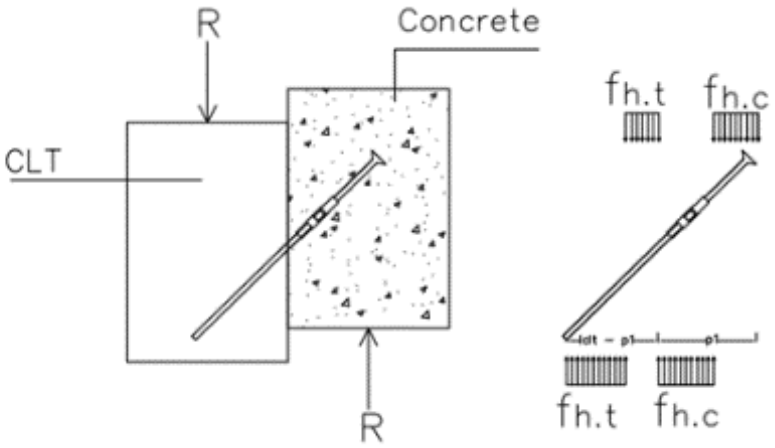

Figure 18. Failure mode 1.

2. Failure mode with one plastic hinge formation

The ultimate capacity in Mode II is reached when plastic hinge is formed. But with the condition that timber section doesn't fail i.e. the fastener behaves as stiff member in the section (Eq. 27,28) (Figure 19).

$$R_2 = \frac{f_{h,t,0.90} \cdot d_{rod} \cdot l_{concrete}}{2+\beta} \cdot \left(\sqrt{\frac{4 \cdot M_y \cdot \beta^2 \cdot (2+\beta)}{f_{h,t,0.90} \cdot {l_{concrete}}^2 \cdot d_{rod}} + 2 \cdot \beta \cdot (1+\beta)} - \beta \right) [kN] \text{ (Eq.27)}$$

Plastic moment of the rod:

$$M_y = 0.3 \cdot f_{uk} \cdot (d_{rod})^{2.6} [N \cdot mm] \text{ (Eq.28)}$$

f_{uk} *−plastic resistance of the rod [N/mm²]*

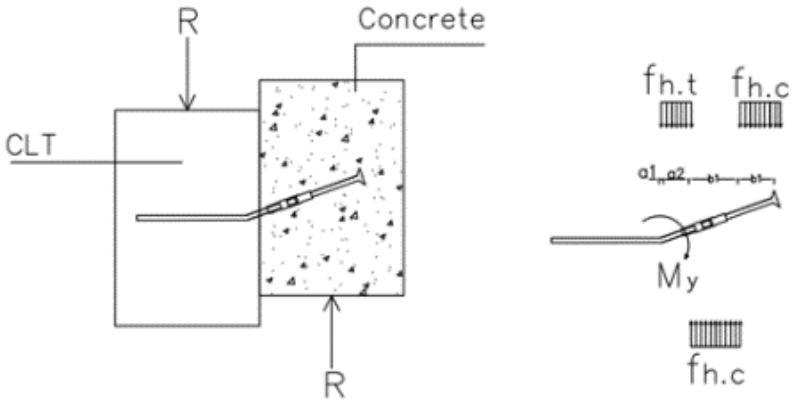

Figure 19. Failure mode 2.

3. Failure mode with two plastic hinges formation

In this failure mode embedment stresses along the road are distributed so that additional plastic hinge is formed (Eq.29) (Figure 20).

$$R_3 = \sqrt{\frac{4 \cdot M_y}{(1+\beta) \cdot \beta \cdot d_{rod} \cdot f_{h,t,0.90}}} [kN] \quad \text{(Eq.29)}$$

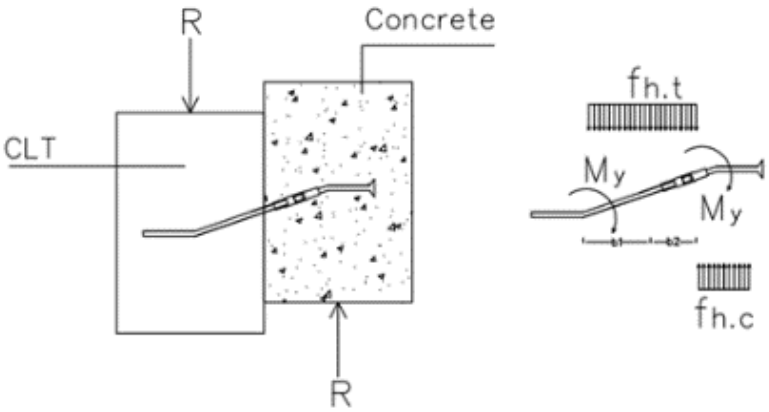

Figure 20. Failure mode 3.

4.2.1 Dowel action

According to the failure modes calculation results it was concluded that the lowest ultimate value arises in failure mode with two plastic hinges accompanied by the vertical displacement (δ). Afterwards the slab is carried by dowel action of the rods (Figure 21).

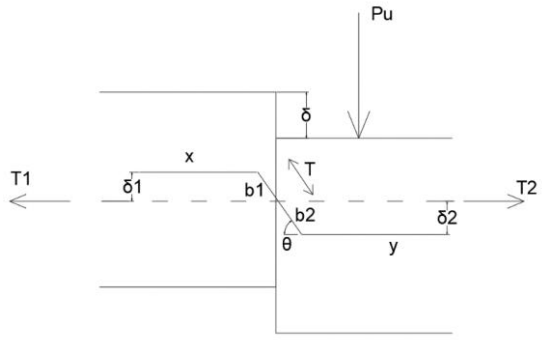

Figure 21. Dowel action schema.

In order to determine the tensile forces acting on rod (T_1 and T_2) in accidental situations the angle θ is to be computed. This can be done by accounting the relative elongation of the rod in the timber-concrete interface, by means of the following equations (Eq.30-42):

$$R_3 = T \cdot \sin\theta \ [kN] \text{ (Eq.30)}$$

$$T = A_{rod} \cdot E_{rod} \cdot \varepsilon \ [kN] \text{ (Eq.31)}$$

$$\sin\theta = \frac{\delta}{b_1+b_2} \ [-] \text{ (Eq.32)}$$

$$\varepsilon = \frac{x+y}{l_{rod}} \ [-] \text{ (Eq.33)}$$

x − length of undeformed embedded in concrete segment

$$x = \frac{b_1-b_1\cdot\cos\theta}{\cos\theta} \ [mm] \text{ (Eq.34)}$$

y − length of undeformed glued in CLT segment

$$y = \frac{b_2-b_2\cdot\cos\theta}{\cos\theta} \text{ (Eq.35)}$$

Where:

$$b_2 = \sqrt{\frac{4\cdot M_y}{(1+\beta)\cdot d_{rod}\cdot f_{h.t.0}\cdot\beta}} \ [mm] \text{ (Eq.36)}$$

$$b_1 = \beta \cdot b_2 [mm] \text{ (Eq.37)}$$

Then the formula (Eq.33) can be written in a form (Eq.38):

$$\varepsilon = \frac{(1-\cos\theta)\cdot(b_1+b_2)}{l_{rod}\cdot\cos\theta} \ [-] \text{ (Eq.38)}$$

After simplifying the previous equations, the formula (Eq.39) is obtained:

$$\cos\theta \cdot \sqrt{1 - 2 \cdot \cos\theta + 2 \cdot \cos\theta^3 - \cos\theta^4} = \frac{R_3 \cdot l_{rod}}{n_{rod} \cdot (b_1 + b_2) \cdot A_{rod} \cdot E_{rod}} \text{ (Eq.39)}$$

Finally, after derivation angle θ can be computed, afterwards tension of rod in accidental situations can be released using equation (Eq.40):

$$T_1 = T_2 = T = R_3 \cdot \cot\theta \ [kN] \text{ (Eq.40)}$$

Then the tensile force is compared with pull-out resistances of both components, with consideration of decreased anchorage length due failure of the rod:

$$l_{CLT.fail} = l_{CLT} - b_2 \ [mm] \text{ (Eq.41)}$$

$$l_{concrete.fail} = l_{concrete} - b_1 [mm] \text{ (Eq.42)}$$

4.2.2 Pull-out stiffness

Stiffness of the connector is an important aspect since it is responsible for gap appearance in the interface between CLT slab and SCC; besides, displacement of the slab can lead to beam ledge overload.
The axial stiffness (K_{III}) of GIR was evaluated by Koets and Jorissen (2012) using the following expression (Eq.43):

$$\frac{1}{K_I} + \frac{1}{K_{II}} = \frac{1}{K_{III}} \ [N/mm] \text{ (Eq.43)}$$

The GIR is divided into two segments K_I (glued-in segment) and K_{II} (the outer part) which are assumed to be interconnected springs (Figure 22).

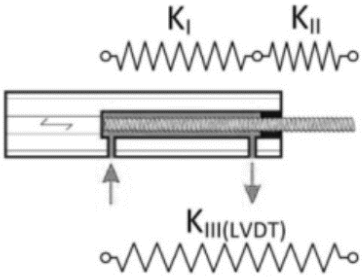

Figure 22. Springs representing GIR connection.

K_I (also denoted as G_f) for PUR and EPX obtained from test results carried by Koets and Jorissen have the following values:

$$G_{f.EPX} = 1200 \ [\frac{N \cdot m}{m^2}]$$
$$G_{f.PUR} = 2200 \ [\frac{N \cdot m}{m^2}]$$

K_{II} is computed using formula (Eq.42):

$$K_{II} = \frac{E_{rod} \cdot A_{rod}}{l_{concrete}} \ [N/mm] \text{ (Eq.44)}$$

Where:
E_{rod} *– modulus of elasticity of the rod [N/mm²]*
$l_{concrete}$ *– length of set in concrete segment [mm]*
A_{rod} *– cross-section area of rod [mm²]*

$$A_{rod} = \frac{\pi \cdot {d_{rod}}^2}{4} \ [mm^2] \text{ (Eq.45)}$$

d_{rod}*– dimeter of the rod [mm]*

4.2.3 Pull-out strength: Glued-in segment

The pull-out strength of the connection is determined by the weakest component, thus possible failure modes are to be investigated. Axially loaded GIR can experience the following failure modes (Tlustochowicz, 2011):

1. Rod yield failure

Behavior of axially loaded rod is described by the formula (Eq.46) (Figure 23):

$$F_{Rd.1} = f_{y.d} \cdot A_{rod} \ [kN] \text{ (Eq.46)}$$

$f_{y.d}$*– design yield strength of steel [N/mm²]*

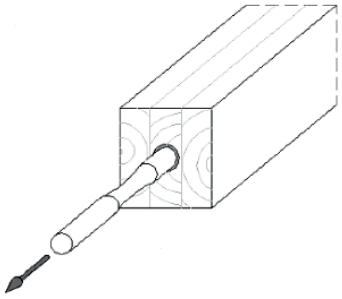

Figure 23. Rod yield failure.

2. Tensile failure of timber cross section

Occurs in perpendicular to the grain loaded rods. The failure can be easily avoided by applying sufficient geometry for wooden board(-s) in which the rod is inserted. The failure mode can be estimated using equation (Eq.47) (Figure 24):

$$F_{Rd.2} = f_{t.0.d.C24} \cdot A_{CLT.board}\ [kN]$$ (Eq.47)

With:

$f_{t.0.d.C24}$ – *tensile strength of wood in parallel to the grain direction [N/mm²]*

$A_{CLT.board}$ – *cross-sectional area of a single board [mm²]*

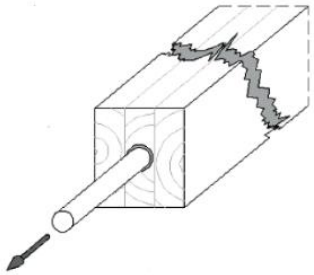

Figure 24. Tensile failure of timber cross section.

3. Splitting failure of the wood

Splitting failure may occur due to short a distance between the rod and the edge of the slab. This failure may be avoided by following the Uibel and Blass provisions (2007) regarding the minimum edge distance (Figure 25).

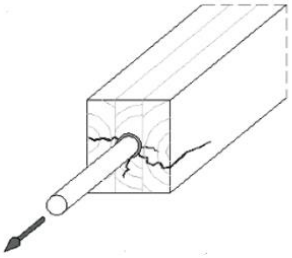

Figure 25. Failure mode 3.

4. Shear failure along the rod (Figure 26)

a. Shear failure of adhesive lines

b. Shear failure of wood

Failure modes 1-3 are easy to predict and avoid, while the shear failure of wood or adhesive has a more complex nature. Pull out capacity is reached when stress along the rod exceeds the maximum stress values of either adhesive or wood. Investigation of this failure mode can be done using Volkerson (1938) shear lag theory (Figure 26).

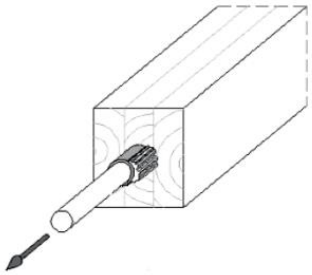

Figure 26. Failure mode 4.

a. Shear failure of adhesive bond lines

Pull-out capacity based on adhesive bond lines shear strength can be computed using the following expressions (Eq.48-52):

$$R_{ax.glue} = \pi \cdot d_{equ} \cdot \tau_{glue.mean} \cdot \frac{tanh(\omega_{\perp,\parallel} \cdot l_{CLT})}{\omega_{\perp,\parallel}} \; [kN] \text{ (Eq.48)}$$

Where:

d_{equ}– equivalent diameter numerically equal to the hole diameter; calculated as (Eq.49):

$$d_{equ} = 1.25 \cdot d_{rod}[mm] \text{ (Eq.49)}$$

$\tau_{glue.mean}$– mean blue shear strength; the value can be estimated according to formulas proposed by Bengtsson and Johannsson (2002):

$$\tau_{mean.PUR} = \min(6.3, 10.3 \cdot {d_{rod}}^{-0.17} \cdot {l_{CLT}}^{-0.08} \cdot {\rho_{CLT}}^{0.45}) \; [\frac{N}{mm^2}]$$
(Eq.50)

$$\tau_{mean.EPX} = \min(8, 10.3 \cdot {d_{rod}}^{-0.52} \cdot {l_{CLT}}^{-0.62} \cdot {\rho_{CLT}}^{0.45}) \; [N/mm^2]$$
(Eq.51)

Factor $\omega_{\perp}$ or $\omega_{\parallel}$ (stresses obtained perpendicularly and paralelly to grain direction respectively) consider the stress dirstribution along the rod:

$$\omega_{\perp,\parallel} = \sqrt{\frac{G_f \cdot \pi}{t_g} \cdot \left(\frac{1}{E_{rod} \cdot A_{rod}} + \frac{1}{E_{0,90.d} \cdot A_{CLT.board}}\right)} \; [\frac{1}{m}] \text{ (Eq.52)}$$

$E_{0,90.d}$– *timber modulus of elasticity [N/mm²]*

b. Shear plug failure

Shear failure of wood is described by the following expressions (Eq.53-55):

$$R_{ax.glue} = \pi \cdot d_{equ} \cdot f_{vd.0,90} \cdot \frac{\tanh(\omega_{\perp,\parallel} \cdot l_{CLT})}{\omega_{\perp,\parallel}} \ [kN] \text{ (Eq.53)}$$

As wood has lower strength properties against stresses obtained in perpendicular to grain direction, the shear resistance must be reduced by applying factor k_{90} as follows:

$$f_{vd.90.C24} = \frac{f_{vd.C24}}{k_{90} \cdot \sin(\alpha)^2 + \cos(\alpha)^2} \ [N/mm^2] \text{ (Eq.54)}$$

$$k_{90} = 1.35 + 0.15 \cdot d_{rod} \ [-] \text{ (Eq.55)}$$

Shear strength of glue is higher than that of timber, thus cohesion failure of wood is likely to occur. Besides, shear strength parallel to the grain is approximately two times greater than the one perpendicular to fibre growth direction; installation of the rod in parallel to grain orientation provides more effective performance of glued-in segment.

4.2.4 Pull-out strength: Embedded in concrete segment

Pull-out strength is calculated by dividing the stud into the components and searching for the weakest, which will represent the axial capacity. These components are described by equations (Eq.56-65) (Figure 27):

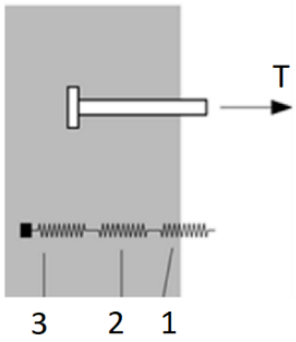

Figure 27. Axially loaded stud schema.

Component 1:

$$N_{Rd,1} = A_{rod} \cdot \frac{f_{uk}}{\gamma_{Ms}} \ [kN] \text{ (Eq.56)}$$

f_{uk} – charactersistic ultimate strength of shaft material of the headed stud [N/mm^2]

Component 2:

$$N_{Rd,p} = p_{uk} \cdot \frac{A_h}{\gamma_{Mc}} \ [kN] \text{ (Eq.57)}$$

p_{uk} – characteristic ultimate bearing pressure at the stud head [N/mm^2]

A_h *– area of the head of the headed stud* (Eq.58)

$$A_h = \frac{\pi}{4} \cdot \left({d_h}^2 - {d_{rod}}^2 \right) [mm^2] \text{ (Eq.58)}$$

$\mathrm{d_h}$ *– diameter of the stud head [mm]*

Component 3:

Concrete cone failure.

$$N_{Rd,c} = N_{0,Rk.c} \cdot \psi_{A.N} \cdot \psi_{s.N} \cdot \frac{\psi_{re.N}}{\gamma_{Mc}} \; [kN] \text{ (Eq.59)}$$

$\psi_{re.N} = 1$

$N_{0,Rk.c}$ *–characteristic resistance of a single anchor without edge and spacing effects*

$$N_{0,Rk.c} = k \cdot {l_{concrete}}^{1.5} \cdot {f_{ck}}^{0.5} \; [kN] \text{ (Eq.60)}$$

$k-$ *basic factor 8.9 for cracked concrete and 12.7 for non-cracked concrete*

$\psi_{A.N}$ *–factor considering geometric effects of spacing and edge distance*

$$\psi_{A.N} = \frac{A_{c,N}}{A^0_{c,N}} \; [-] \text{ (Eq.61)}$$

$\mathrm{A_{c,N}}$ *–actual projected area of the cone*

$$A_{c,N} = \frac{\pi \cdot {d_c}^2}{4} \; [mm^2] \text{ (Eq.62)}$$

Where:

$$d_c = 2 \cdot l_{concrete} \cdot \tan(\alpha) + d_h \; [mm] \text{ (Eq.63)}$$

$\alpha = 55 \; deg$

$A^0_{c,N}$ *–is reference area of the concrete cone of an individual anchor with large spacing and edge distance projected on the concrete surface [mm²]*

$$A^0_{c,N} = \frac{9 \cdot \pi \cdot {l_{concrete}}^2}{4} \; [mm^2] \text{ (Eq.64)}$$

Factor accounting for the influence of edges of the concrete member on the distribution of stresses in concrete:

$$\psi_{s.N} = 0.7 + 0.3 \cdot \frac{c}{c_{cr,N}} [-] \text{ (Eq.65)}$$

Where:

$$c = 1.5 \cdot l_{concrete} \; [mm]$$
$$c_{cr,N} = 0.5 \cdot s_{cr,N} \; [mm]$$

4.3 **Execution of rods**

4.3.1 Minimum spacing

Based on the German design code (DIN1052) the minimum spacing between the rods and edge distances should meet the following criteria (Table 4):

Table 4. Minimum spacing.

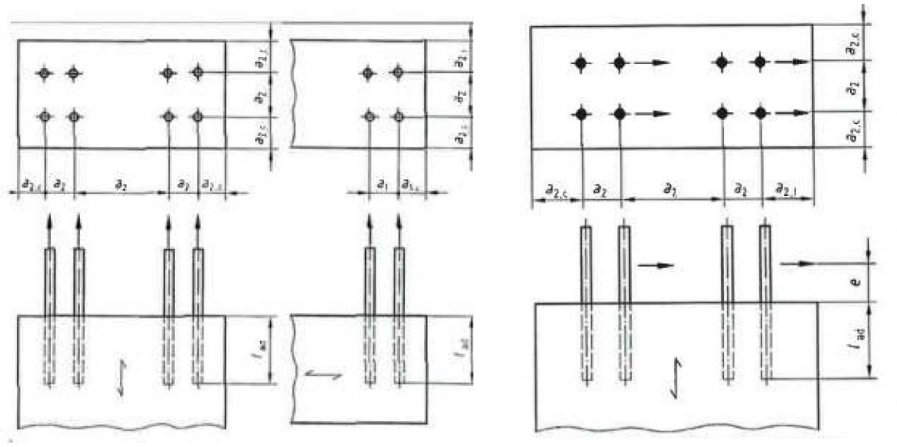

GIR direction	parallel to fibre		perpendicular to fibre			
Minimum distance	a_2	$a_{2,c}$	a_1	$a_{1,c}$	a_2	$a_{2,c}$
	5*d	2,5*d	4*d	2,5*d	4*d	2,5*d

4.3.2 Installation

The quality of adhesive bond lines can be affected by shrinkage during hardening, sensitivity to elevated temperatures and moisture content, and limited gap-filling quality during installation process. Since the ambient conditions assumed to be constant with time, the gap-filling quality is the main objective of the thesis.

There are two main ways for GIR installation. Since most adhesives perform better with thin glue-lines, then the drilled hole should be equal to 1.25 of rod diameter (Eurocode). After the hole is drilled and cleaned of saw dust, adhesive is poured inside and then the rod can be inserted; the rod extrudes the glue along the rod as shown in the picture (Figure 28).

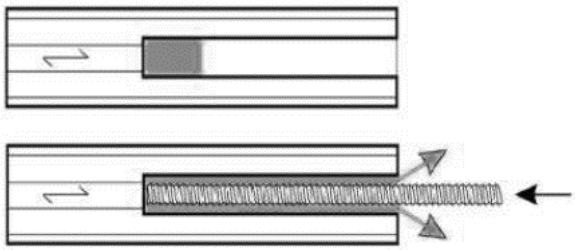

Figure 28. Method 1.

The disadvantage of this method is that it doesn't guarantee that the glue is distributed uniformly and there are no unfilled cavities or voids.
A more reliable gluing technique requires additional holes drilled perpendicular to the main one. When the rod is placed and the main hole is plugged, adhesive is injected under pressure through the one of the additional holes. Injection continuous till the glue is extruded through the other hole (Figure 29).

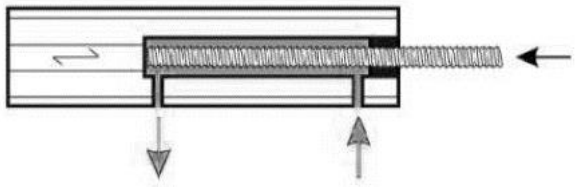

Figure 29. Method 2.

4.3.3 Recesses

Recesses in narrow face of the CLT must be sawn in order to provide access to the couplers during erection stage. The minimum distance between the rod and the edge surface is 40 mm, which allows to avoid unfilled cavities and provides enough space for fastening the couplers (Figure 30). While the minimum depth of a recess (*d)* is calculated as follows (Equation 66):

$$d = H_{CLT} \cdot tan\theta \ [mm] \quad \text{(Eq.66)}$$

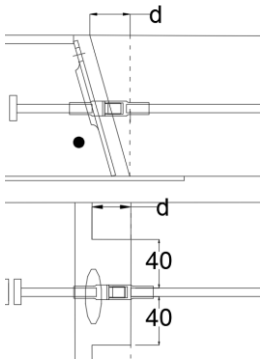

Figure 30. Recesses in slab.

4.3.4 Use limitation

According to Uibel and Blass (2007) the following limitations must be considered (Figure 31):

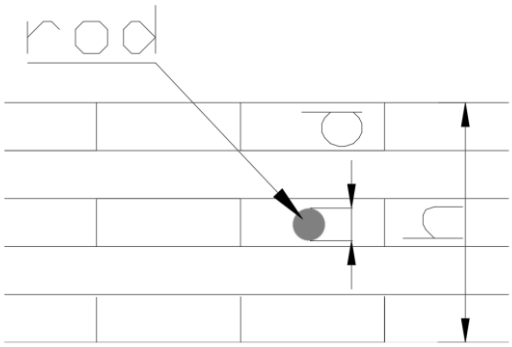

Figure 31. Limitation.

- Advised position is parallel to the grain
- Height of the slab (min $h = 6 \cdot d$)

5 STUD WELDED TO STEEL PLATE

5.1 **Description**

The connector has a wide range of appliance as GIR, while remaining rather cheap. The given connector type is more sustainable on case of accidental situations as fire, since screws are less sensitive to elevated temperature than glued connections.

The joint consists of Headed stud (described in 4.4), MODIX® coupler, steel plate and screws. There are two variations of this connections which are distinguished in the way they are fastened to CLT slab (Figures 32-34):

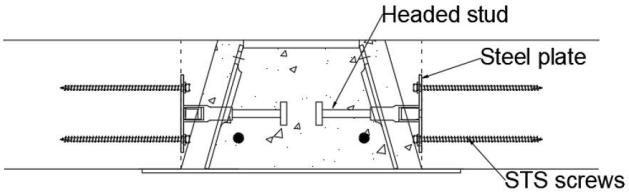

Figure 32. Narrow face connector.

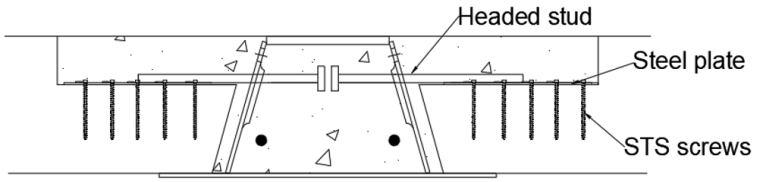

Figure 33. Main face connector I.

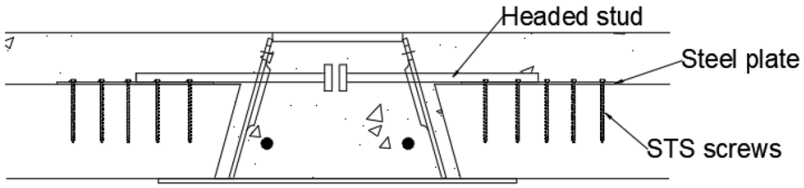

Figure 34. Main face connector II.

5.2 **Screws**

Screwed connections are the most common way of joining timber with other structural elements as steel and concrete. Screwed connections are used in 60% of cases in CLT structures (Brandner & Schickhofer, 2014), this prevalence is due to the high reliability and low price of the fasteners.

5.2.1 Pull-out resistance

The axial characteristic withdrawal capacity of fully threaded self-tapping screw (STS) is determined using formula based on test results governed by Uibel and Blass (2007). The formula takes into consideration the angle between the screw axis and grain direction and characteristic density of layer in which screw is inserted (Figure 35) (Equation 66).

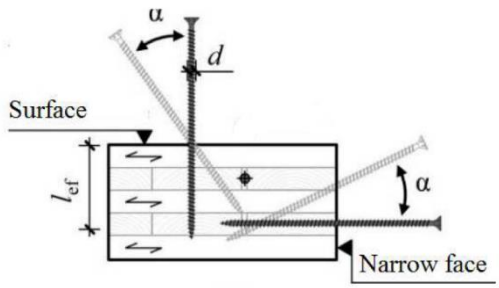

Figure 35. Designation for screws positions.

$$R_{ax,s,k} = \frac{0.35 \cdot d_{screw}^{0.8} \cdot l_{ef}^{0.9} \cdot \rho_k^{0.75}}{1.5 \cdot \cos^2\alpha + \sin^2\alpha} \; [kN] \quad \text{(Eq.66)}$$

With:

d_{screw} *−nominal screw diameter [mm]*
l_{ef} *−effective penetration depth [mm]*
ρ_k *−characteristic density of CLT [kg/m³]*
α *−angle between the screw axis and CLT grain direction: 90° on the main surface, 0° narrow face [deg]*

While tensile load carrying capacity can be determined using basic equation (Eq.67):

$$\mathrm{R_{ax,k}} = \frac{f_{u,k} \cdot \pi \cdot (0.6 \cdot d_{screw})^2}{4} \; [kN] \text{ (Eq.67)}$$

$f_{u,k}$ *−ultimate tensile stress [N/mm²]*

5.2.2 Pull-out stiffness

The stiffness of axially loaded screw can be estimated by means of the following formula obtained by Blass (2006). The formula (Eq.68) considers diameter of a screw, its effective length and the average density of the slab:

$$K_{ser.ax} = 234 \cdot {\rho_{CLT}}^{0.2} \cdot {d_{screw}}^{0.2} \cdot {l_{ef}}^{0.4} \; [N/mm] \text{ (Eq.68)}$$

5.2.3 Lateral resistance

Load bearing capacity of laterally loaded screw is dependent upon CLT embedment strength. As embedment strength of a screw inserted in the main face concerns the entire cross-section, and the embedding strength in the narrow face concerns only relevant layers, thus different characteristic densities must be considered.

Main surface:

$$f_{h,CLT,k} = 0.0112 \cdot {d_{screw}}^{-0.5} \cdot {\rho_{CLT}}^{1.05} \; [N/mm^2] \text{ (Eq.69)}$$

ρ_{CLT} *=400 kg/m³*

Narrow face:

$$f_{h,CLT,k} = 0.862 \cdot {d_{screw}}^{-0.5} \cdot {\rho_{CLT}}^{0.56} \; [N/mm^2] \text{ (Eq.70)}$$

ρ_{CLT} =350 kg/m³

The shear resistance is represented by the smallest Johansen failure mode value:

$$M_{y,Rk} = 0.3 \cdot f_{y,d} \cdot {d_{screw}}^{2.6} \; [kN \cdot m] \text{ (Eq.71)}$$

$$F_{v.Rd} = min\begin{cases} f_{h,CLT,k} \cdot l_{eff} \cdot d_{screw} \\ f_{h,CLT,k} \cdot l_{eff} \cdot d_{screw} \cdot \left(\sqrt{2 + \frac{4 \cdot M_{y,Rk}}{f_{h,CLT,k} \cdot {l_{eff}}^2 \cdot d_{screw}}}\right) \\ 2.3 \cdot \sqrt{M_{y,Rk} \cdot f_{h,CLT,k} \cdot d_{screw}} + \frac{R_{ax,s,k}}{4} \end{cases}$$ (Eq.72)

5.2.4 Strength of inclined screws

Shear resistance of inclined screw is a sum of tension and shear resistance previously defined (5.2.1 and 5.2.3 respectively); the final equation for the inclined screw is the following (Hossain et.al., 2018):

$$R_v = \mathrm{R_{ax,k}} \cdot \cos\beta + F_{v.Rd} \cdot \sin\beta \ [N/mm^2]$$ (Eq.73)

β −angle between screw axis and the CLT

5.2.5 Stiffness of inclined screws

The stiffness of the inclined screw is calculated as per formula (axial and lateral stiffnesses were defined in 5.2.2 and 3.1.2 respectively) (Eq.74):

$$K_{inc} = \sqrt{{K_{ser.ax}}^2 + {K_{ser}}^2}\ N/mm$$ (Eq.74)

5.2.6 Effective number of screws

According to Eurocode 1995, the resistance of a connection to a group of screws is determined by using a statically effective number of screws. For the axially loaded screws the effective number of screws is determined as (Eq.75):

$$n_{eff} = n^{0.9}[\text{-}]$$ (Eq.75)

When the laterally loaded screws are inserted into the narrow face, the effective number of screws depends on the spacing between the fasteners. For screws inserted into the main surface of the CLT slab, reducing the statically effective number of fasteners is not required (Table 5).

Table 5. Number of effective screws.

n_{eff}	In narrow face	In surface
Withdrawal	$n^{0,9}$	$n^{0,9}$
Shearing-off	$n^{0,85}\ (a_1 \geq 10 \cdot d)$ $n^{0,9}\ (a_1 \geq 14 \cdot d)$	n

5.2.7 Screws placing

According to Uibel and Blass (2007) in order to avoid splitting failure of wood, the minimum requirements for spacing, edge and end distances should be fulfilled (Table 6).

Table 6. Number of effective screws.

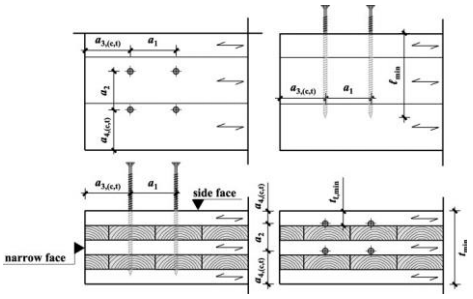

	Narrow face	Main surface
a1	10*d	4*d
a3,t	12*d	6*d
a3,c	7*d	6*d
a2	3*d	2,5*d
a4,t	6*d	6*d
a4,c	3*d	2,5*d

5.3 **Weld resistance**

A headed stud or part of a coupler are joined to a steel plate by welding. According to Eurocode 1993-1-8 the design resistance of the fillet weld may be assumed adequate if, at every point along its length, the resultant of all the forces per unit length transmitted by the weld satisfy the following criteria (Eq. 76):

$$\max\left(T_{Ed}, V_{Ed}\right) \leq l_{weld} \cdot a \cdot \frac{f_u}{\sqrt{3} \cdot \beta_w \cdot \gamma_{M2}} \text{ (Eq.76)}$$

Where:

a −throat thickness of the weld [mm]
f_u −nominal ultimate tensile strength [N/mm^2]
β_w −correlation factor [-]
γ_{M2} −partial safety factor [-]
l_{weld} −weld length [mm]

For narrow face weld length calculated as (Eq.77):

$$l_{weld} = \pi \cdot \left(a \cdot \sqrt{2} + d_{stud}\right) \text{ [mm] (Eq.77)}$$

d_{stud} −stud diameter [mm]

5.4 **Steel plate**

5.4.1 Tension resistance

The resistance of the plate is described by the minimum resistance of three possible plastic collapse mechanisms (Figure 36) (Eq. 78).

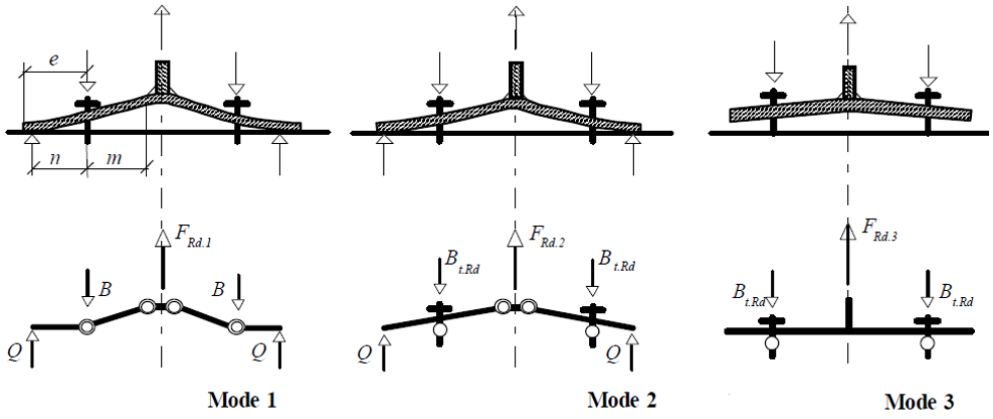

Figure 36. Plate failure modes.

$$min\begin{cases}\frac{4\cdot l_{eff}\cdot M_{pl.Rd}}{m}\\ \frac{2\cdot l_{eff}\cdot M_{pl.Rd}+n_{screw.ef}\cdot F_{t.Rd}}{m+n}\\ n_{screw.ef}\cdot F_{t.Rd}\end{cases} \quad \text{(Eq.78)}$$

5.4.2 Shear resistance

Shear resistance of the steel plate is checked in accordance with Eurocode 1993-1-1 (Eq.79).

$$F_{pl.Rd} = \frac{k_1\cdot\alpha_b\cdot d_{screw}\cdot t_{pl}\cdot f_u}{\gamma_{M2}}\ [kN] \quad \text{(Eq.79)}$$

Where:

$$\alpha_b = min\begin{cases}\frac{e_1}{3\cdot d_{screw}}\\ \frac{p_1}{3\cdot d_{screw}}-0.25\\ 1\end{cases} \qquad k_1 = min\begin{cases}2.8\cdot\frac{e_2}{d_{screw}}-1.7\\ 1.4\cdot\frac{p_2}{d_{screw}}-1.7\\ 2.5\end{cases}$$

Where e_1, e_2, p_1 and p_2 (Figure 37) are the minimum spacing according to Eurocode 1993. Spacing requirements for p_1 and p_2 are not compatible with CLT ones, thus minimum spacings for the p values have to be taken from Table 6 (5.2.7).

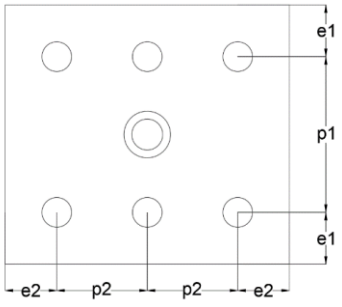

Figure 37. Holes location schema.

6 OSB SCREWED PLATE

6.1 Description

Oriented splice board (OSB) is set over the beam top plate and fastened to the face side of the slab by screws (Figure 38). The connection is cheap, but the appliance is limited to intermediate beams.

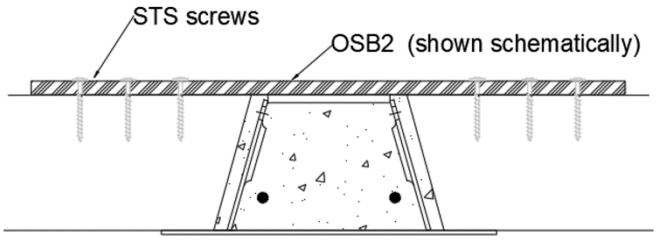

Figure 38. OSB screwed plate.

6.2 Plate design

The characteristic load-carrying capacity of a panel-to-timber connection shall be calculated with the equations where the thickness of the wood-based panel is at least according to equation (Eq.80-84):

$$t_{OSB} \geq \sqrt[1.2]{1.6 \cdot (1.1 \cdot d_{screw})^{1.6}}\ [mm] \text{ (Eq.80)}$$

Bending, shear and tension resistances of the OSB plate must satisfy the requirements stated in Eurocode 1995-1-1 (6.1.6, 6.1.7 and 6.1.3 respectively) (Eq.81):

$$\sigma_{t,d} \leq f_{t,d} \text{ (Eq.81)}$$

Where:
$\sigma_{t,d}$ *−design tensile stress [N/mm²]*
$f_{t,d}$ *−design tensile strength [N/mm²]*

$$\frac{\sigma_{m,y,d}}{f_{m,y,d}} + \frac{\sigma_{m,z,d}}{f_{m,z,d}} \leq 1 \text{ (Eq.83)}$$

$\sigma_{m,y,d}\ and\ \sigma_{m,z,d}$ *−design bending stresses about the principal axes [N/mm²]*
$f_{m,y,d}\ and\ f_{m,z,d}$ *−corresponding design bending strengths [N/mm²]*

$$\tau_d \leq f_{v,d} \text{ (Eq.84)}$$

τ_d *−design shear stress [N/mm²]*
$f_{v,d}$ *−design shear strength [N/mm²]*

6.3 **Pull-through resistance**

The vertical movement is resisted by OSB plate, so that screws are simultaneously subjected to both shear and pull-out actions.
According to Eurocode 1995-1-1 the head pull-through resistance is estimated as follows (Eq.85):

$$F_{Rd} = \pi \cdot \left(\left(\frac{1}{2} \cdot d_{screw,h}\right)^2 - \left(\frac{1}{2} \cdot d_{screw}\right)^2\right) \cdot 3 \cdot f_{c,90,k}\ [kN] \quad \text{(Eq.85)}$$

$d_{screw,h}$ *−diameter of screw head [mm]*
d_{screw} *−screw diameter [mm]*

7 TRANSVERSE REINFORCEMENT

Transverse ribbed reinforcing bars are used for joining the composite floor and SCC beam (Figure 39). Further design of connection assumes full shear interaction between the timber and concrete composite sections.

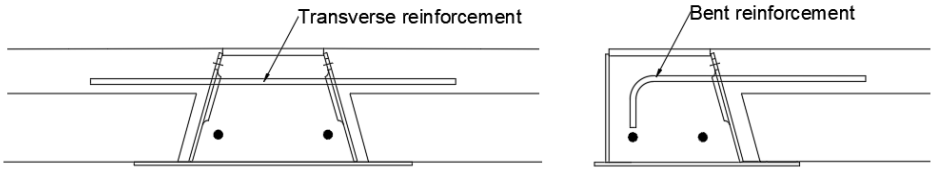

Figure 39. Transverse reinforcement.

7.1 **Anchorage length**

Straight or bent depends reinforcement can be used for joining floor slab and the DELTABEAM® (Figure 40). Tension capacity of such connector depends upon anchorage length, that can be computed using formulas (Eq.86-87):

$$l_{b,rqd} = \frac{d_{rebar} \cdot \sigma_s}{4 \cdot 2.25 \cdot \eta_1 \cdot \eta_2 \cdot f_{ctd}}\ [mm] \quad \text{(Eq.86)}$$

d_{rebar} *−diameter of rebar*
σ_s *−stress in reinforcement*

$$l_{b,eq} = \alpha_1 \cdot l_{b,rqd}\ [mm] \quad \text{(Eq.87)}$$

α_1 *−factor for bent reinforcement*

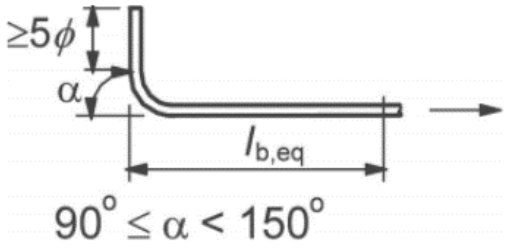

Figure 40. Bent reinforcement.

7.2 **Shear resistance**

Shear resistance of the connection can be estimated as follows (Eq. 88-89):

$$V_{Rd} = 0.21 \cdot (100 \cdot \rho_1)^{\frac{1}{3}} \cdot H_{con} \cdot 1m \; [kN] \text{ (Eq.88)}$$

$$\rho_1 = \frac{A_{rebar} \cdot n_{rebar}}{H_{con} \cdot 1m} \; [-] \text{ (Eq.89)}$$

H_{con} −thickness of concrete cover layer [mm]
A_{rebar} −cross section area of rebar [mm^2]
n_{rebar} −bumber of rebars [-]

7.3 **Crack width control**

The crack width control ensures that the obtained crack will not be wide enough for hazard interaction of the reinforcing bars with ambient conditions (high relative humidity etc.), which could lead to strength loss caused by rusting. The acceptable width of crack should not exceed the limit of 0.3 mm (XC1; Eurocode 1992-1-1). The crack width can be obtained by the following set of formulas (Eq.90-94):

$$w_k = s_{r,max} \cdot \varepsilon_{cr} \; [mm] \text{ (Eq.90)}$$

Where:

$$s_{r,max} = 3.4 \cdot c_c + 0.425 \cdot \frac{k_1 \cdot k_2 \cdot d_{rebar}}{\rho_{p.eff}} \; [mm] \text{ (Eq.91)}$$

k_1 −coefficient of rebar bond property
k_2 −coefficient of strain distribution
c_c −concrete cover

$$\varepsilon_{cr} = \frac{\sigma_s - k_t \cdot \frac{f_{ct.eff}}{\rho_{p.eff}} \cdot \left(1 + \frac{E_S}{E_{cm}} \cdot \rho_{p.eff}\right)}{E_s} \; [-] \text{ (Eq.92)}$$

$$\rho_{p.eff} = \frac{A_{rebar} \cdot n_{rebar}}{\min\left(0.5 \cdot H_{con}, 2.5 \cdot (c_c + 0.5 \cdot d_{rebar}), \frac{H_{con} - x}{3}\right)} \ [mm] \text{ (Eq.93)}$$

x −deapth of neutral axis [mm]

$$f_{ct.eff} = 0.3 \cdot f_{ck}^{\frac{2}{3}} \ [N/mm^2] \text{ (Eq.94)}$$

8 CASE STUDIES

Both case studies are consisting of three parallel beams (2xDR-beams; 1xD-beam), supporting CLT slabs as shown below (Figure 41, 42):

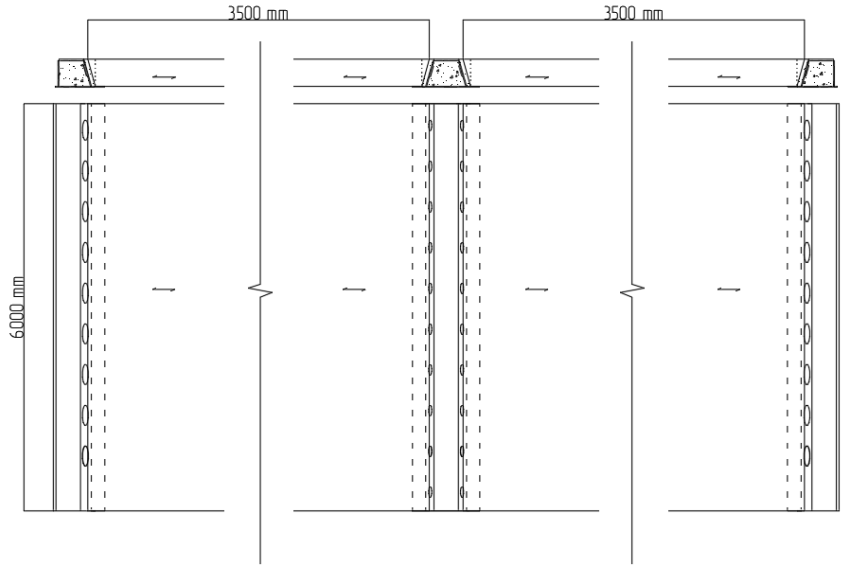

Figure 41. Study case without concrete topping.

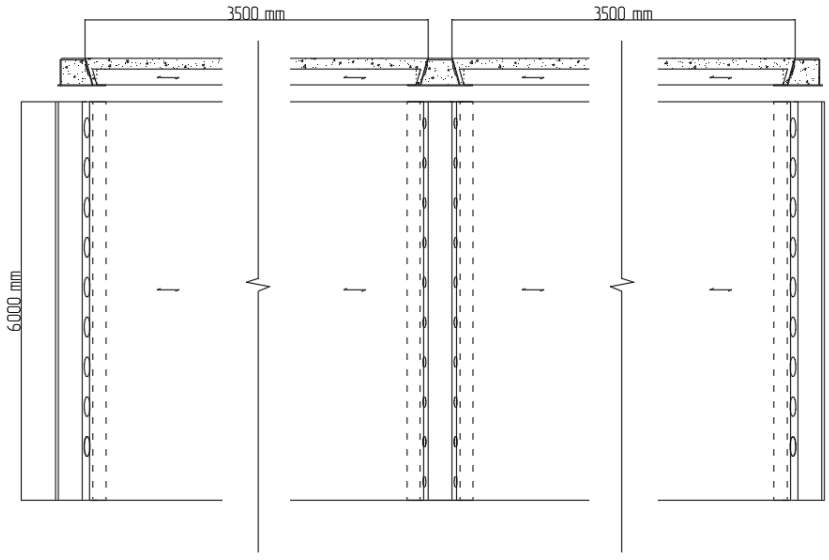

Figure 42. Study case with concrete topping

Geometric properties of the slabs used for case studies are (Table 7):

Table 7. CLT board pattern; L-parallel to span, C-perpendicular.

Case	CLT slab	L [mm]	C [mm]	L [mm]	C [mm]	L [mm]	H [mm]
I	L5s	40	40	40	40	40	200
II	L5s	30	20	30	20	30	120+80 (topping)

While the dimensions of the beams are performed below (Table 8) (Figure43):

Table 8. DELTABEAM® geometry.

Case	Composite beam	h [mm]	d2 [mm]	b1 [mm]	b2 [mm]	b [mm]	B [mm]
I	D20-300	200	5	97,5	100	200	495
II	DR20-245	200	5	100	180	245	365

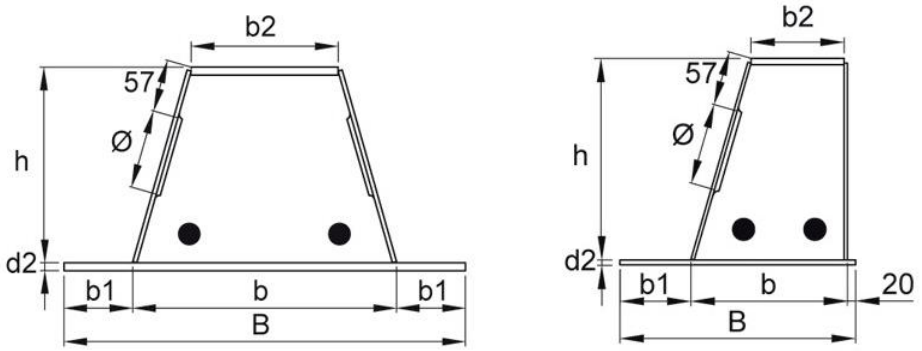

Figure 43. DELTABEAM® geometry D- and DR- beams.

8.1 **Loads**

8.1.1 Load cases

Domestic residential (A) load category was considered (Acc. EN1990) (Table 9):

Table 9. Imposed loads.

Categories of loaded areas	q_k [kN/m^2]	Q_k [kN]
Category A	1.5 to 2	2 to 3
Category B	2 to 3	1.5 to 4.5
Category C1	2 to 3	3 to 4
Category C2	3 to 4	2.5 to 7 (4)
Category C3	3 to 5	4 to 7
Category C4	4 to 5	3.5 to 7
Category C5	5 to 7.5	3.5 to 4.5

The properties of the case studies are the following:

- Consequence class: CC2, XC1
- Lifetime category: 3 (50 years)
- Timber: C24
- Concrete: C20/24
- Fire class: R60

8.1.2 Load combinations

Load duration reduction factors (Acc. EN1990) (Table 10):

Table 10. Reduction factors.

	Ψ_0	Ψ_1	Ψ_2
Category A	0.7	0.5	0.3
Category B	0.7	0.5	0.3
Category C	0.7	0.7	0.6

Load combinations are calculated as follows (Eq.95-100):

SLS combination:

$$W_{SLS} = G_{k1,2} + g_k + q_k \quad \text{(Eq.95)}$$

SLS quasi permanent:

$$W_{SLS.qp} = G_{k1,2} + g_k + \psi_2 \cdot q_k \quad \text{(Eq.96)}$$

ULS combination:

$$W_{ULS} = \gamma_G \cdot G_{k1,2} + \gamma_G \cdot g_k + \gamma_Q \cdot q_k \quad \text{(Eq.97)}$$

ULS fire:

$$W_{ULS.fire} = \gamma_{fi} \cdot G_{k1,2} + \gamma_{fi} \cdot g_k + \psi_1 \cdot \gamma_{fi} \cdot q_k \quad \text{(Eq.98)}$$

$G_{k1,2}$-self-weight of the slab, where:

$$G_{k1} = \rho_{CLT} \cdot H_{CLT} \quad \text{(Eq.99)}$$

$$G_{k2} = \rho_{CLT} \cdot H_{CLT} + \rho_{con} \cdot hH_{top} \quad \text{(Eq.100)}$$

8.1.3 Loads acting on connection

The loads acting on connector can be determined using expressions Eq.101-103:

$$Q_1 = Q_2 = Q = \frac{W \cdot L_{CLT}}{2}\ [kN] \text{ (Eq.101)}$$

$$\mathrm{M}_{Ed} = \frac{W \cdot {L_{CLT}}^2}{8}\ [kN \cdot m] \text{ (Eq.102)}$$

$$V = \frac{Q}{\frac{(cos\theta)^2}{\sin\theta - \mu \cdot cos\theta} + \sin\theta}\,[kN] \text{ (Eq.103)}$$

For the first loading diagram (Figure 44) the loads are (Eq.105-106):

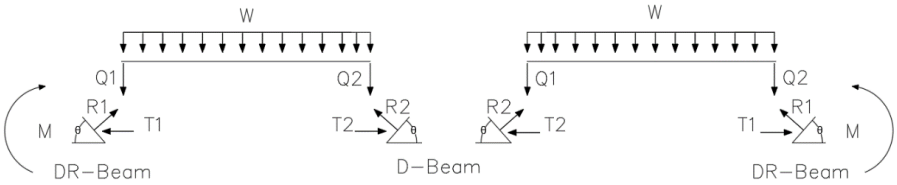

Figure 44. Loading diagram I.

$$T_{Ed1} = Q \cdot \tan\theta\ [kN] \text{ (Eq.105)}$$

$$R_{Ed1} = \frac{Q}{cos\theta}\,[kN] \text{ (Eq.106)}$$

While for the second diagram (Figure 45) the loads are (Eq.107-109):

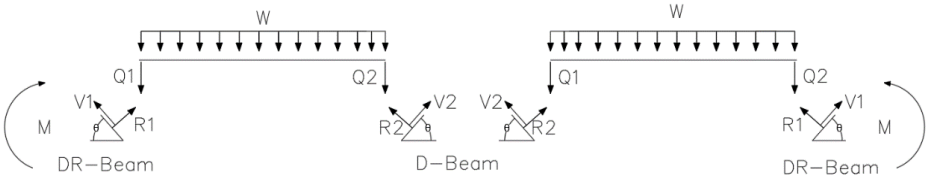

Figure 45. Loading diagram II.

$$V_{Ed} = V \cdot \sin\theta\ [kN] \text{ (Eq.107)}$$

$$T_{Ed2} = V \cdot cos\theta\ [kN] \text{ (Eq.108)}$$

$$R_{Ed2} = \frac{Q - V_{Ed}}{cos\theta}\,[kN] \text{ (Eq.109)}$$

8.1.4 Torsion

Intermediate beams are assumed to be symmetrically loaded, thus those study case beams are not subjected to torsion, while magnitude of torque moment in edge beams must be defined. The exact location of reaction force R is hard to estimate precisely enough, so it is conservatively assumed that the force is applied to that point of the web's surface, where it produces the largest torque moment as shown in Figure 46.

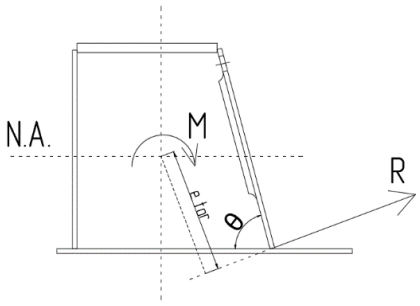

Figure 46. DR-beam, torsion schema.

In order to compute the lever arm e_{tor} that was mentioned in chapter 2.3.2 (Eq.1), the following expression involving composite beam's geometry should be applied (Eq.110-112):

$$e_{tor} = \frac{y_{N.A.}}{\sin\theta} - \frac{h}{6 \cdot \sin\theta} + (x_{N.A.} - y_{N.A.} \cdot \cot\theta) \cdot \cos\theta \; [mm] \quad \text{(Eq.110)}$$

Then the torsional moment is estimated as follows (Eq.111):

$$M = R \cdot e_{tor} \; [kN \cdot m] \quad \text{(Eq.112)}$$

Then for eliminating the torque moment there should be at least two oppositely directed forces: for DR-beams those are Compressive and Tensile forces (Figure 47). Magnitudes and point of application of the force vector depends upon the load acting on slab and slab properties.

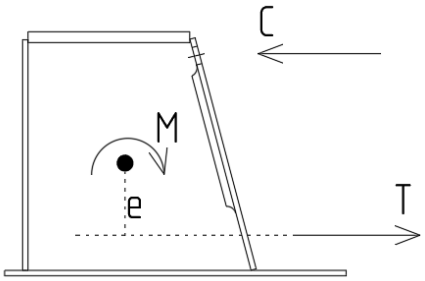

Figure 47. Torsion in DR-beam.

In the first case the torsional moment M is eliminated by the slab (*vector* $\vec{C}$) and the torsion reinforcement (*vector* $\vec{T}$). The position of the vector $\vec{C}$ is the top level of the slab, while the vector $\vec{T}$ location depends on how the torsion reinforcement is set (through the main web hole [depends on beam geometry]; through the additional web hole [at least 75 mm above the bottom plate surface]).

Then the magnitude of the *vector T* is calculated as (Eq.113):

$$T = \frac{M - \frac{h_{CLT} \cdot C}{2}}{e} \; [kN] \quad \text{(Eq.113)}$$

The contribution of the $\vec{C}$ vector is dependent upon the CLT slab's compressive resistance, which should satisfy the following criteria (Eq.114):

$$C < \frac{A_{layer} \cdot f_{c.0}}{\frac{f_{c.0}}{k_{c90} \cdot f_{c.90}} \cdot (sin^2\beta + cos^2\beta)} \text{(Eq.114)}$$

$f_{c.0}$ *−compressive strength parallel to grain [N/mm²]*
I_{CLT} *−second moment of area of the slab [mm⁴]*
R *−reaction force [kN]*

9 DETAIL LIBRARY

Based on the calculation process described and case study assumptions made, the following standard details were obtained as detail drawings.

9.1 Glued-in Discrete Threaded Rod

Connection described in Chapter 4.

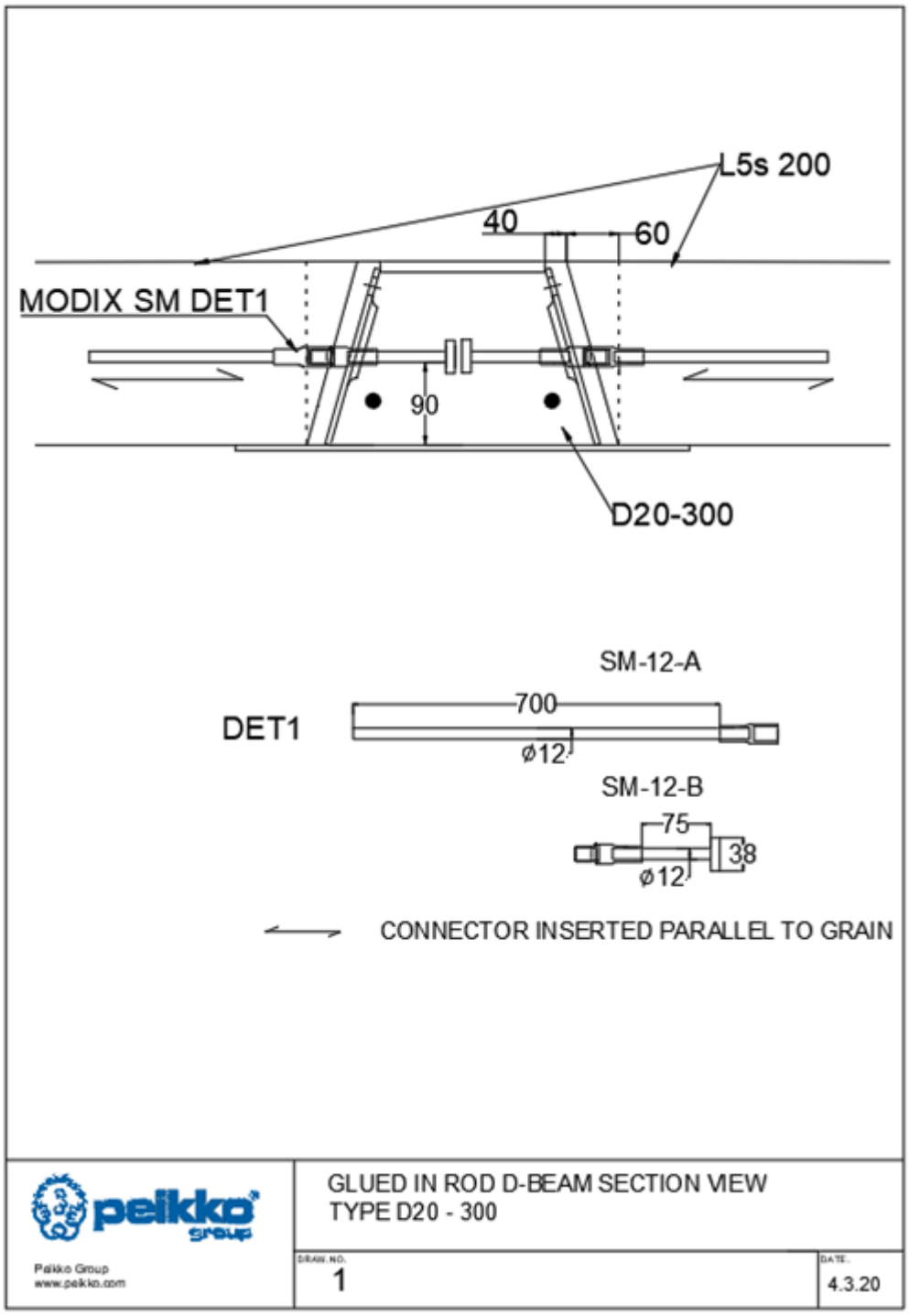

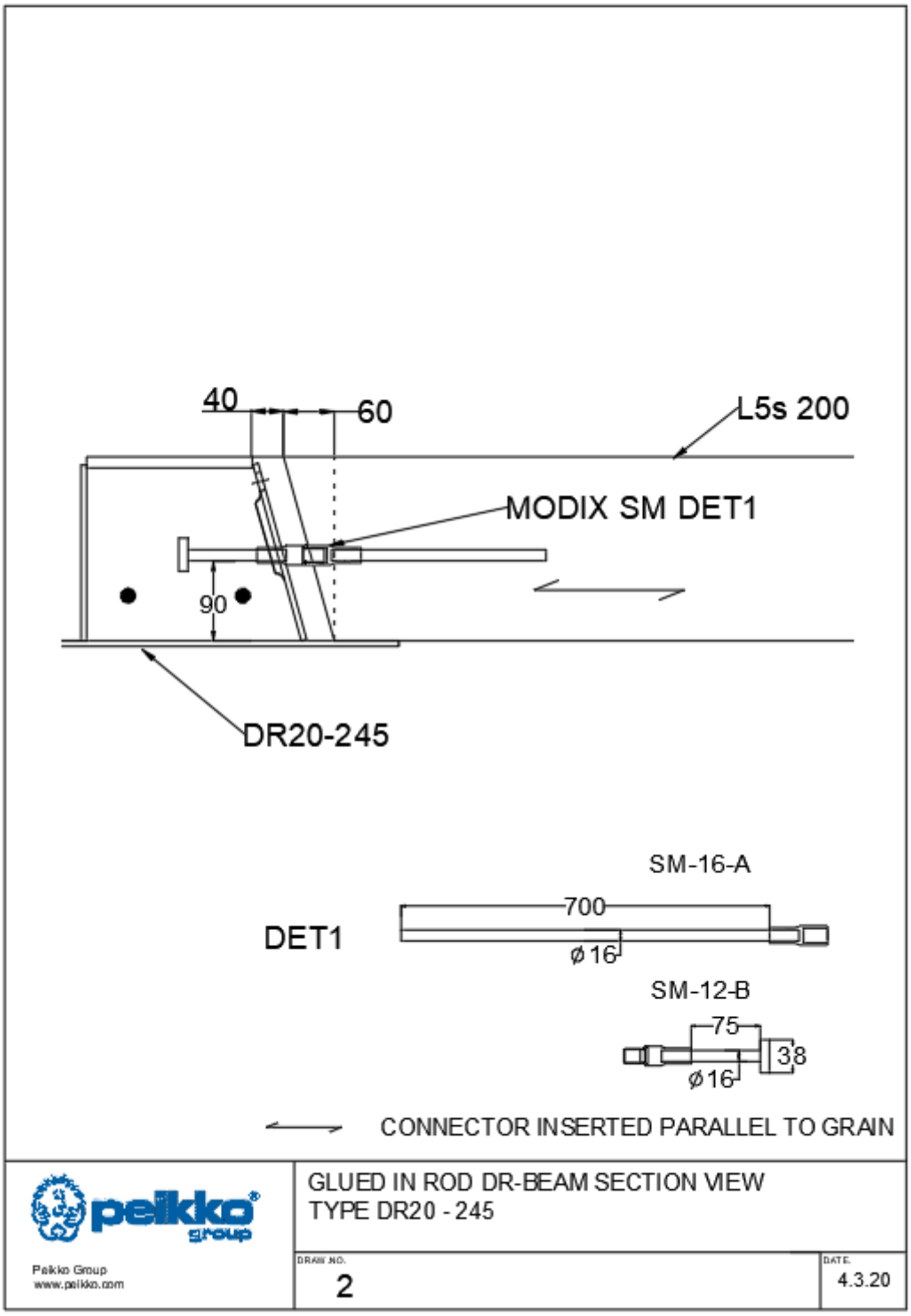
40
60
L5s 200
MODIX SM DET1
90
DR20-245
SM-16-A
DET1
700
ø16
SM-12-B
75
38
ø16
CONNECTOR INSERTED PARALLEL TO GRAIN
Pelkko Group
www.pelkko.com
GLUED IN ROD DR-BEAM SECTION VIEW
TYPE DR20 - 245
DRAW NO.
2
DATE.
4.3.20

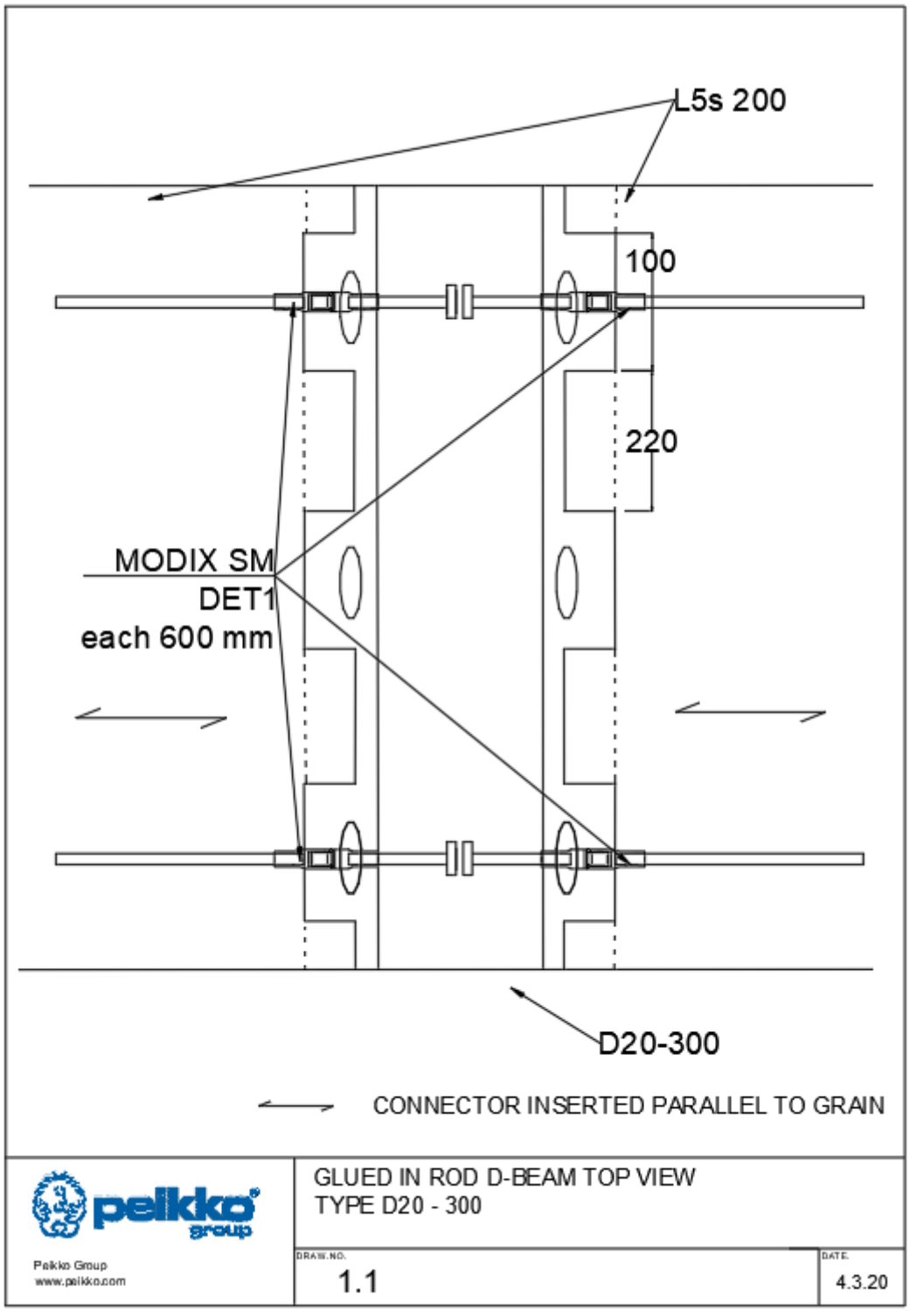
L5s 200
100
220
MODIX SM
DET1
each 600 mm
D20-300
CONNECTOR INSERTED PARALLEL TO GRAIN
pelkko group
Pelkko Group
www.pelkko.com
GLUED IN ROD D-BEAM TOP VIEW
TYPE D20 - 300
DRAW.NO.
1.1
DATE.
4.3.20

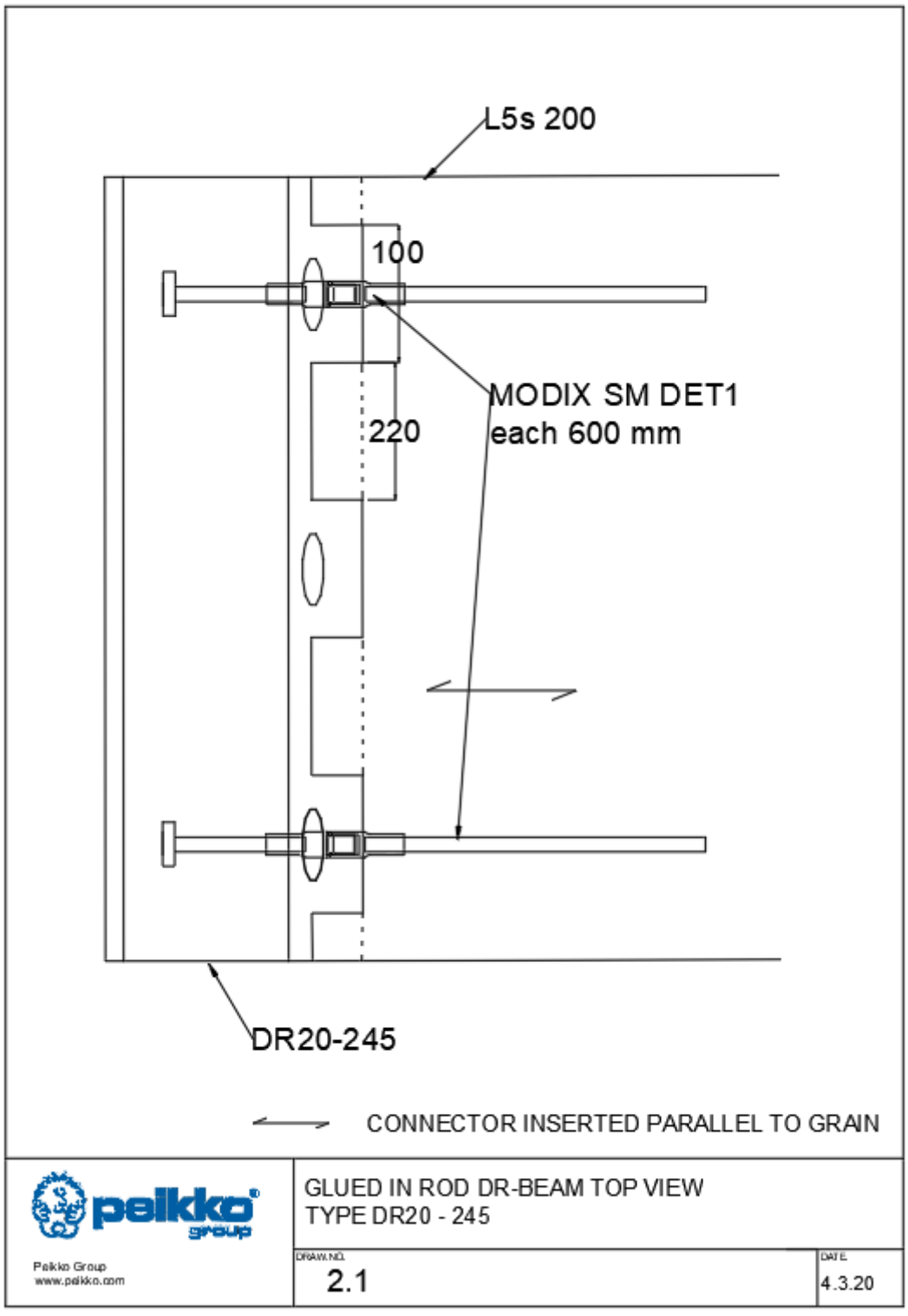
L5s 200
100
MODIX SM DET1
each 600 mm
220
DR20-245
CONNECTOR INSERTED PARALLEL TO GRAIN
Pelkko Group
www.pelkko.com
GLUED IN ROD DR-BEAM TOP VIEW
TYPE DR20 - 245
DRAW.NO.
2.1
DATE
4.3.20

9.2 **Headed studs**

9.2.1 Narrow face

Connection described in Chapter 5.

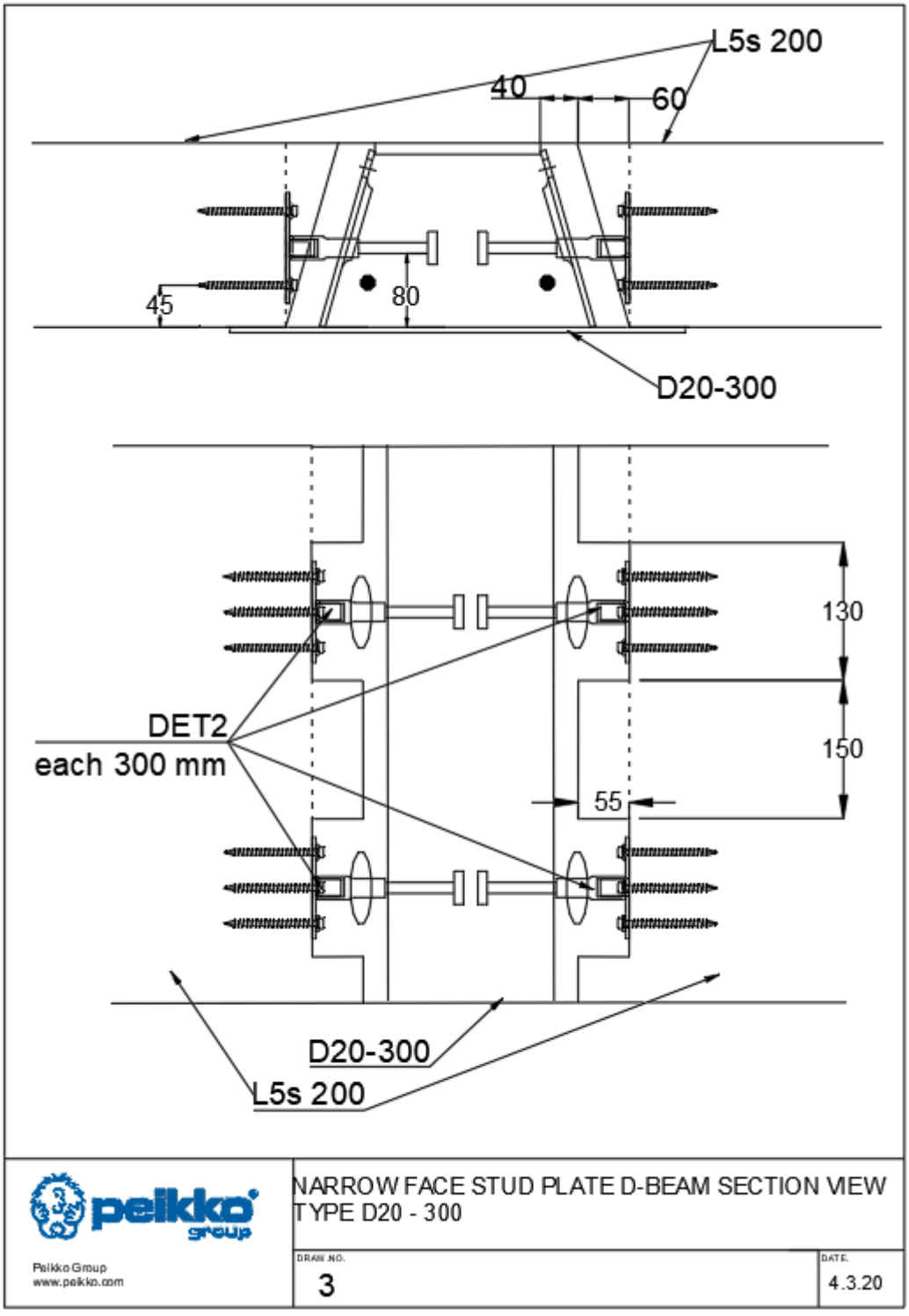

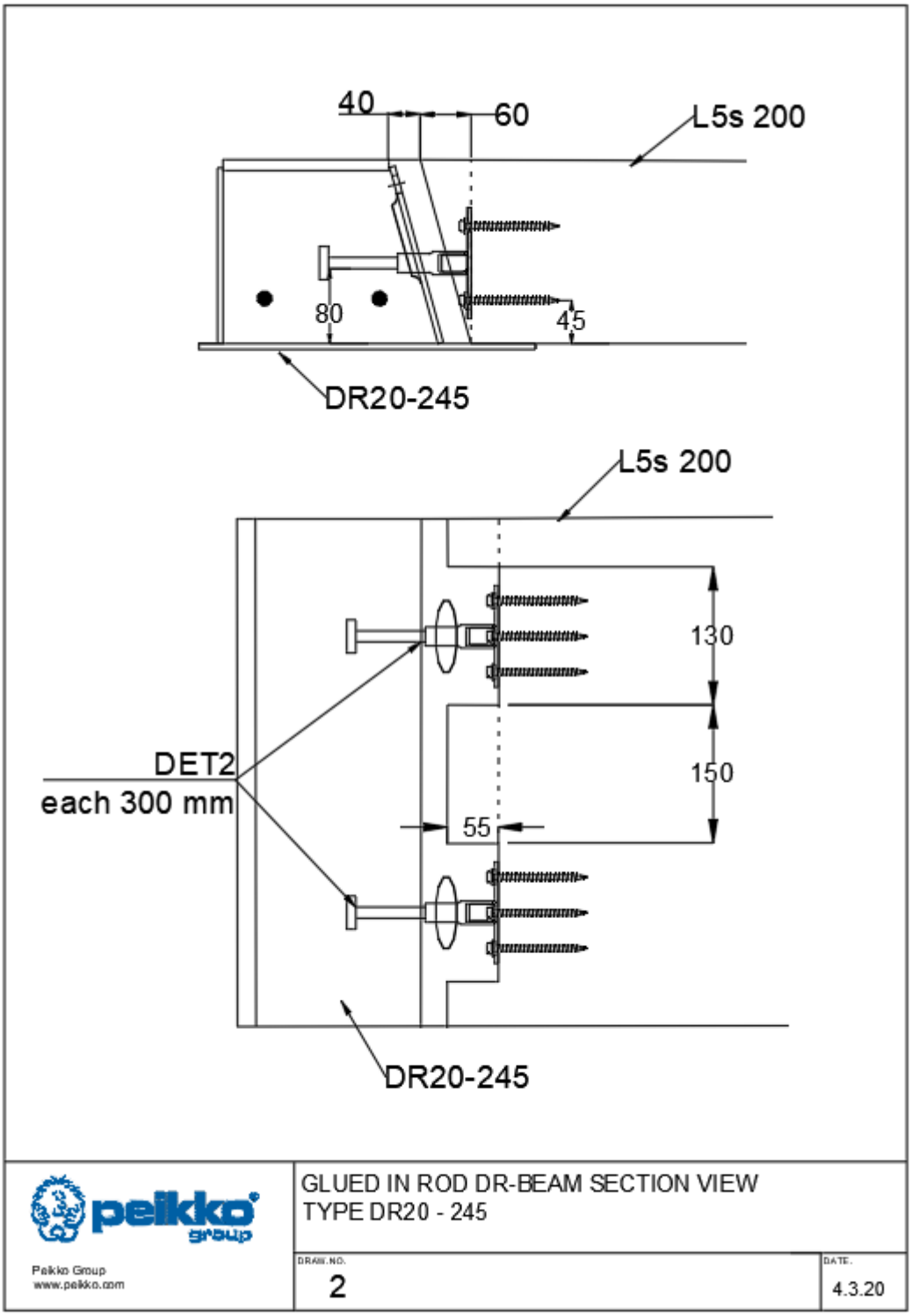

Peikko Group
www.peikko.com

GLUED IN ROD DR-BEAM SECTION VIEW
TYPE DR20 - 245

DRAW. NO.
2

DATE.
4.3.20

9.2.2 Main face

Connection described in Chapter 5.

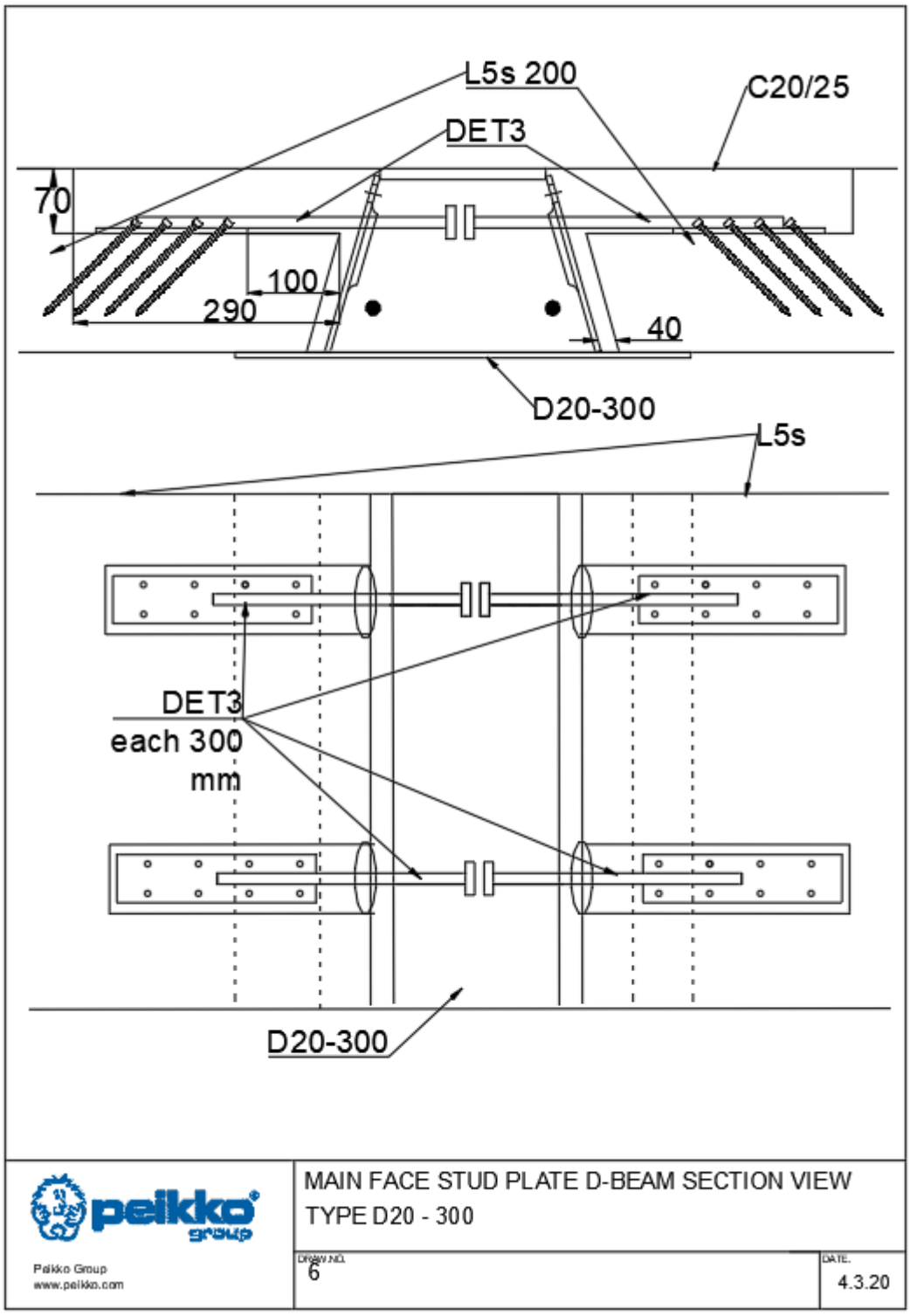

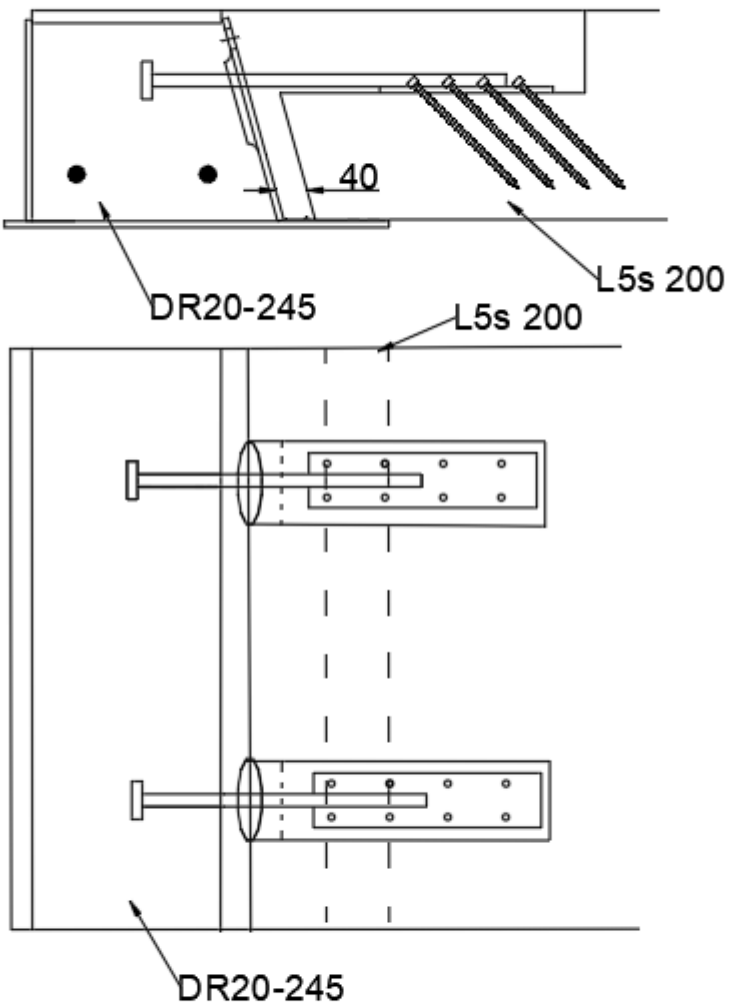

pelkko group

Pelkko Group
www.pelkko.com

GLUED IN ROD DR-BEAM SECTION VIEW
TYPE DR20 - 245

DRAW.NO.
4

DATE
4.3.20

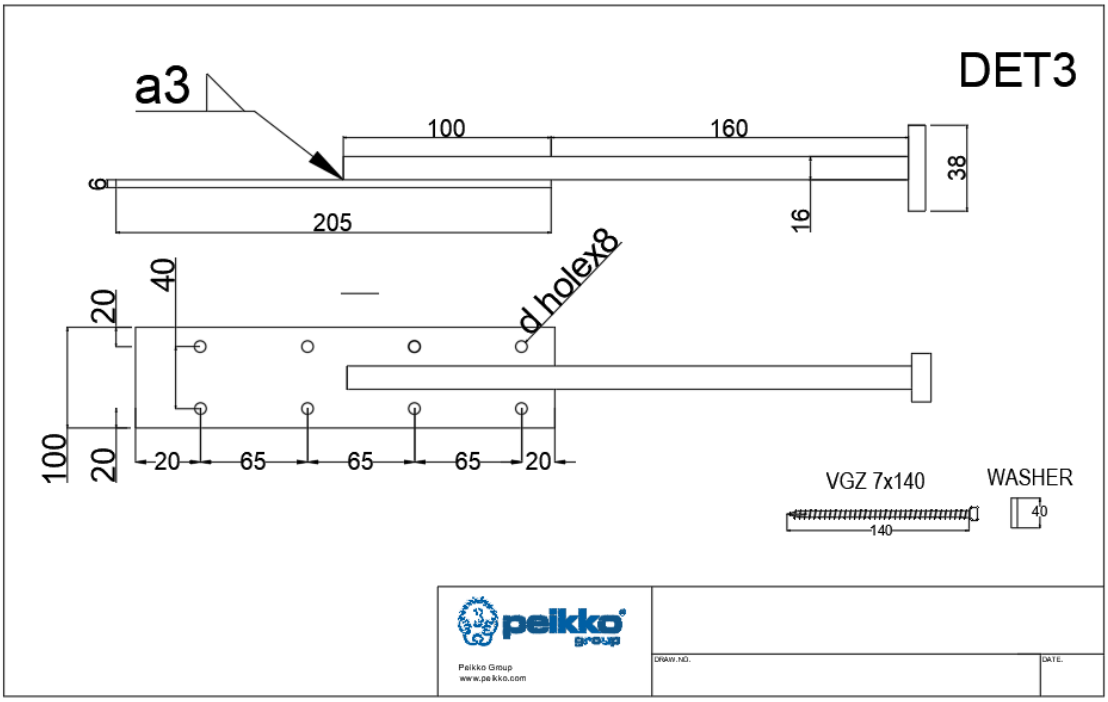
DET3
a3
100
160
38
6
205
16
40
20
d holex8
100
20
20
65
65
65
20
VGZ 7x140
140
WASHER
40
Peikko Group
www.peikko.com
DRAW.NO.
DATE.

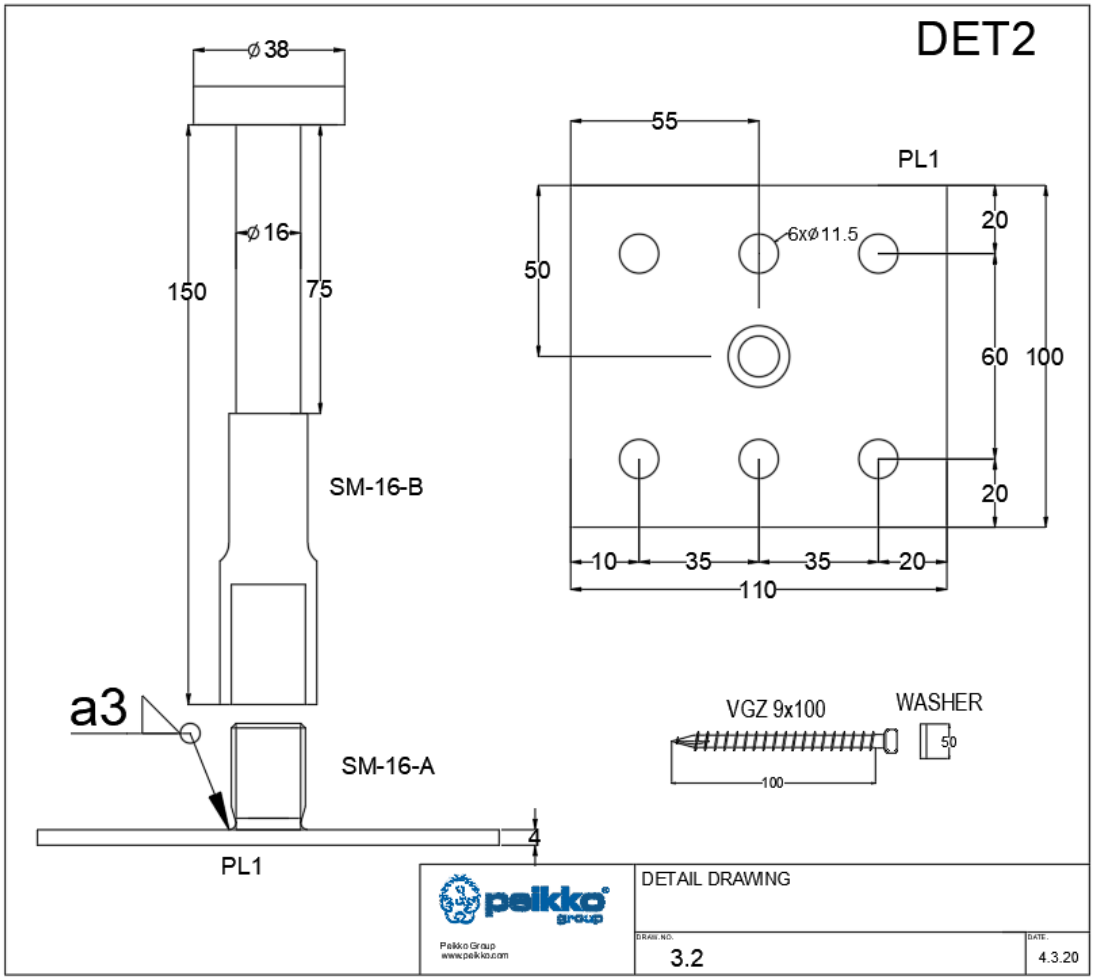
DET2
ø38
ø16
150
75
SM-16-B
SM-16-A
a3
PL1
4
55
PL1
6xø11.5
50
20
60
100
20
10
35
35
20
110
VGZ 9x100
100
WASHER
50
Peikko Group
www.peikko.com
DETAIL DRAWING
DRAW.NO.
3.2
DATE.
4.3.20

9.3 **OSB screwed plate**

Connection described in Chapter 6.

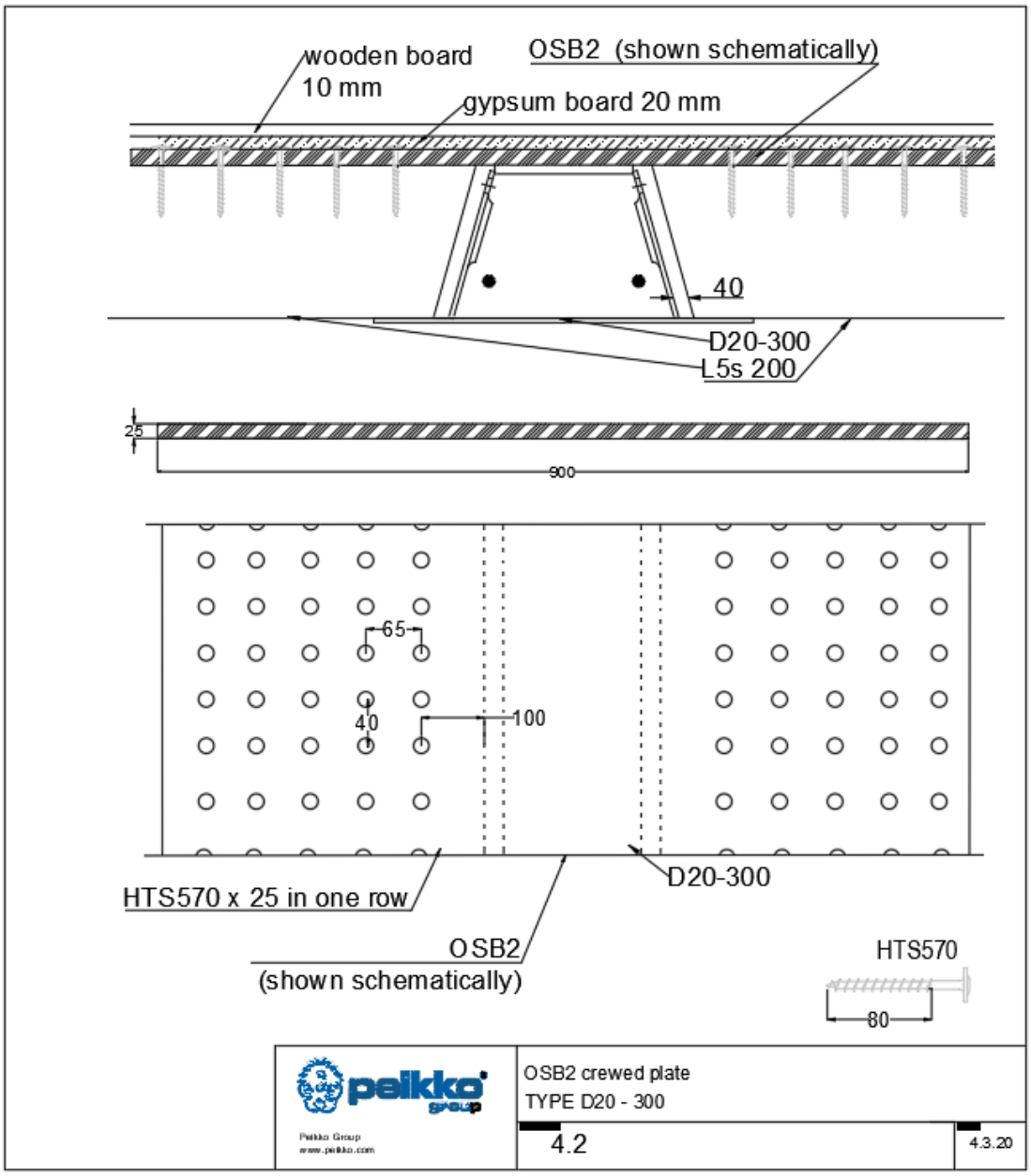

9.4 **Transverse reinforcement**

Connection described in Chapter 7.

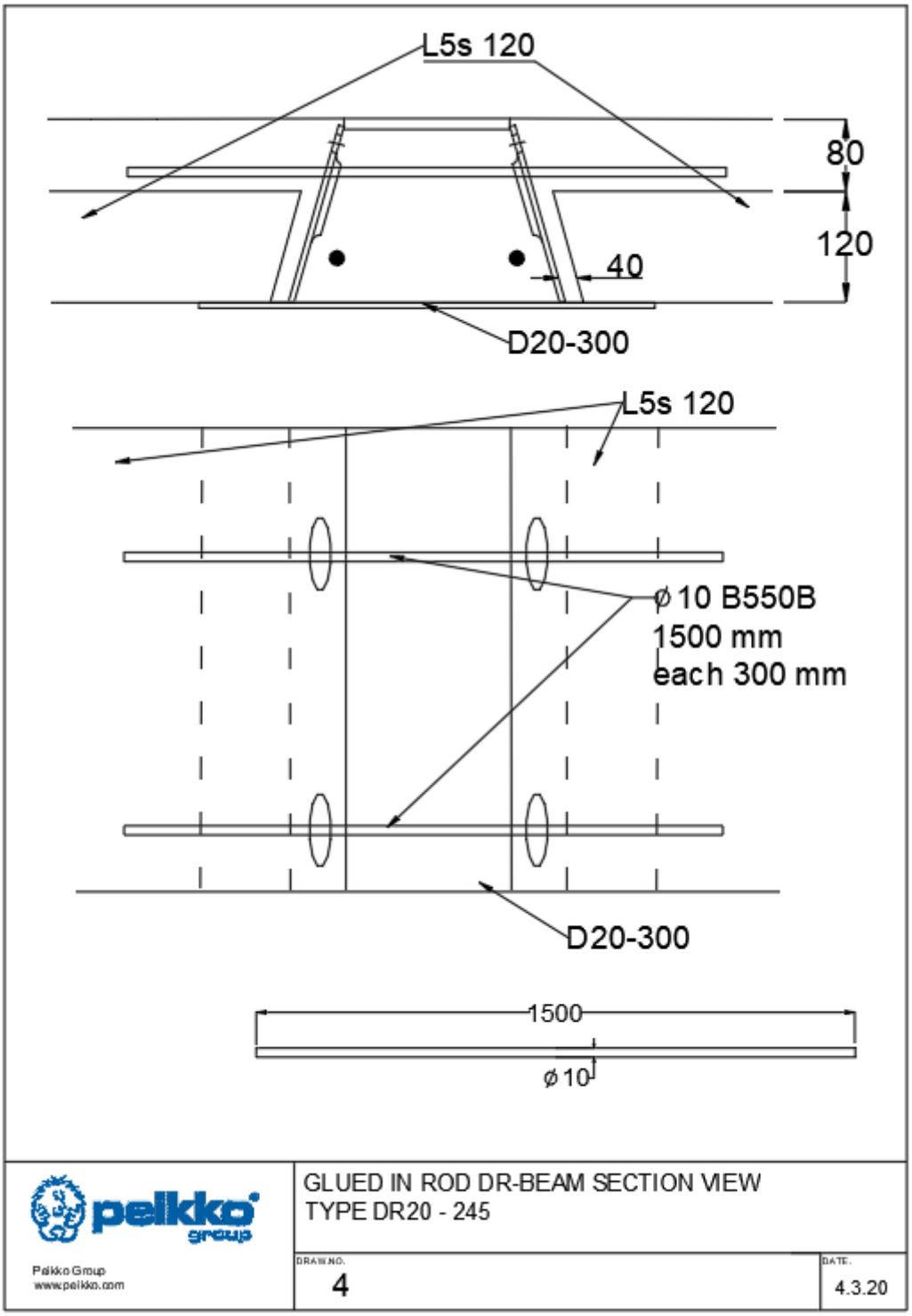

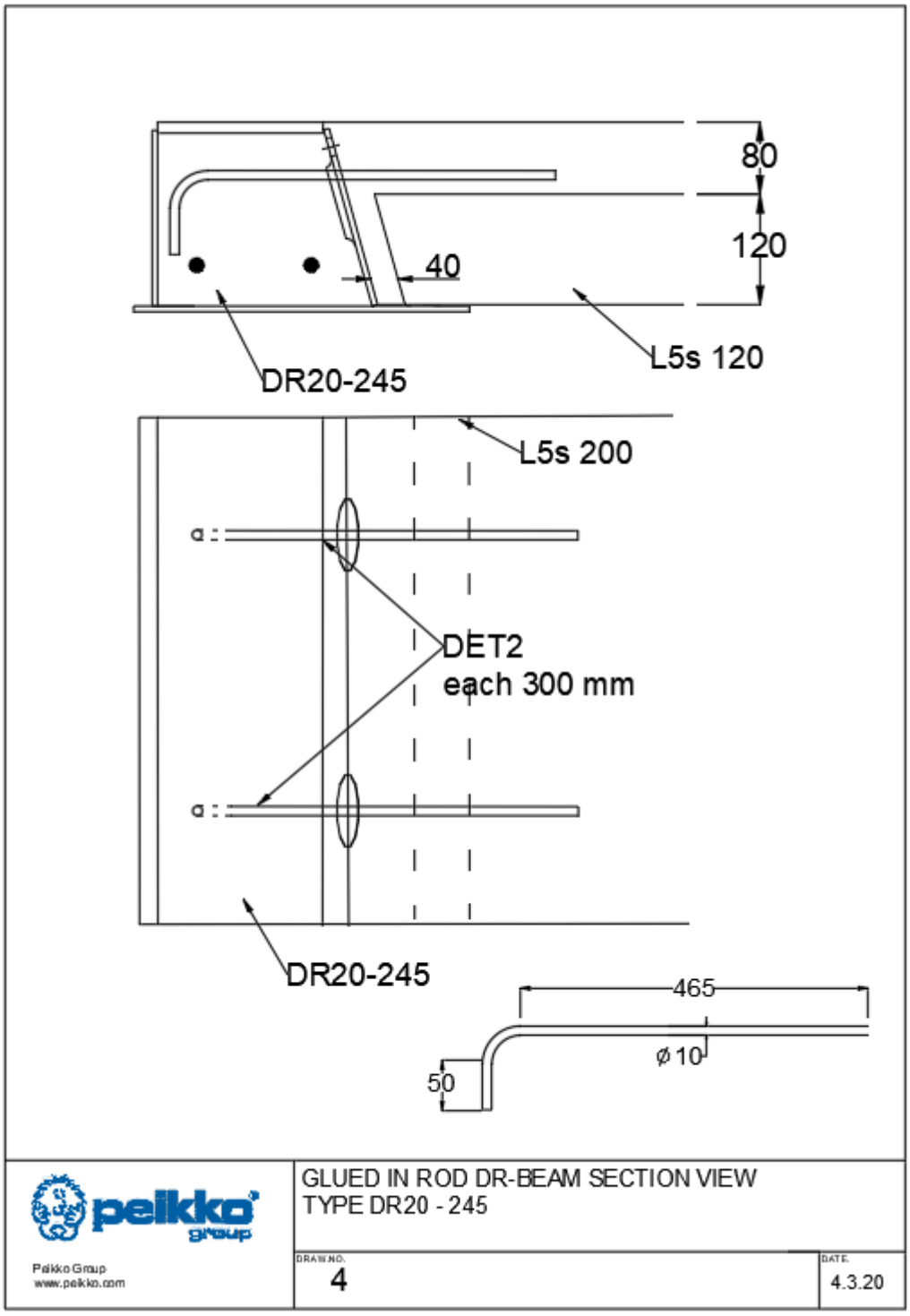
80
120
40
DR20-245
L5s 120
L5s 200
a :
DET2
each 300 mm
a :
DR20-245
465
ø 10
50
GLUED IN ROD DR-BEAM SECTION VIEW
TYPE DR20 - 245
Pelkko Group
www.pelkko.com
DRAWING NO.
4
DATE
4.3.20

10 CONCLUSION

The main goal of the research was achieved, detail library comprising the most common connection details between CLT and SCC beam was created. The general connection details between CLT and SCC beam are hybrid of traditional connections used in timber and concrete structures joined between each other:

- Screws

Axially loaded screws have relatively high strength and stiffness in comparison with laterally loaded ones, thus inclined screws are advisable.

- GIR

GIRs have to be designed so that ductile failure is ensured and risk of sudden failure is diminished. High stiffness of the connector doesn't allow significant gap opening in the interface between the beam and the slab, which is decisive.

GIR connections allow to significantly facilitate erection process by reducing installation time, as far as glued in segment is pre-installed in the CLT slab.

- Headed stud

Headed stud was found one of the main forms of concrete joining connection. The given connector is easy to install, and it reduces the consequences of improper installation (eccentricity, overlapping)

- MODIX® coupler

The given coupler is suitable for interconnection of the joint segments, which significantly facilitates the erection process and allows to benefit from prefabricated connections as GIR, or Studs welded to steel plates.
As a conclusion, it can be said, that the load transfer mechanism between the beam and the slab can be affected in a way that the beam ledge is activated due to connection slip, which can require strengthening of the bottom plate in case of heavily loaded slabs or long spans. Otherwise, the connections in slim-floor composite structures with timber-based flooring (CLT) act according to the same principles as connections used in concrete floors.
Further studies will deal with connection performance in non-constant ambient conditions and more detailed fire design of glued connections.

REFERENCES

Aicher, S. & Dill-Langer, G. (2001). *Effect of Polar Anisotropy of Wood loaded Perpendicular to Grain*. Retrieved 9.10.2019 from https://www.researchgate.net/publication/239391632_Effect_of_Polar_Anisotropy_of_Wood_Loaded_Perpendicular_to_Grain

Bengtsson, C. & Johansson, C. (2002). *GIROD-Glued in rods in timber structures*. Retrieved 11.10.2019 from http://www.diva-portal.org/smash/record.jsf?pid=diva2%3A962224&dswid=6918

Green, D.W., Winandy, J.E. & Kretschmann, D.E. (1999). *Wood handbook—Wood as an engineering material.* Retrieved 12.11.2019 from https://www.fpl.fs.fed.us/documnts/fplgtr/fplgtr113/ch04.pdf

He, G., Xie, L., Wang, X., Yi, J. & Peng, L. (2016). *Timber-concrete structures.* Retrieved 10.11.2019 from https://bioresources.cnr.ncsu.edu/wp-content/uploads/2016/10/BioRes_11_4_9205_He_XWYPC_Shear_Behavior_Timber_Conc_9813.pdf

Hossain, A., Loss C. & Tannert, T. (2018). *Simple Cross-Laminated Timber shear connections with spatially arranged screws*. Retrieved 10.11.2019 from https://www.sciencedirect.com/science/article/pii/S0141029618312446

Jockwer, R. & Steiger, R. (2016). *Performance of Self-Tapping Screws and Threaded Steel Rods in shear reinforcement of glulam beams.* Retrieved 10.11.2019 from file:///C:/Users/zhukopav/Downloads/WCTE2016_Paper_345_Jockwer_Steiger.pdf

Koets, R.J. & Jorissen, A.J.M. (2012). *Experimental investigation of the axial strength of glued-in rods on cross laminated timber*. Retrieved 12.11.2019 from https://link.springer.com/article/10.1617/s11527-018-1268-y

Leskelä, M. (1998). *Joint reinforcement*. Company private document, Peikko Group.

Peikko Group. (2014). *DELTABEAM® Slim Floor Structure Technical manual*. Retrieved 9.10.2019 from https://d76yt12idvq5b.cloudfront.net/file/dl/i/qS6c7g/rRibeblCUQJvj7DtCwoE4w/DELTABEAMPeikkoGroup001TMAWeb.pdf

Peikko Group. (2016). *MODIX® Rebar Coupler technical manual*. Retrieved 8.10.2019 from https://www.peikko.com/products

Rothoblass. (2019). *Screw properties.* Retrieved 1.11.2019 from https://www.rothoblaas.com/products/fastening/screws/screws-carpentry

Brandner, R. & Schickhofer, G. (2014). Screwed Joints in Cross Laminated Timber Structures. Retrieved 3.10.2019 from https://graz.pure.elsevier.com/en/publications/screwed-joints-in-cross-laminated-timber-structures

Stepinac M., Hunger F., Serrano E. & Tomasi R. (2013). *Comparison of design rules for glued-in rods and design rule proposal for implementation in European standards*. Retrieved 9.10.2019 from https://www.researchgate.net/publication/261025694_Comparison_of_design_rules_for_glued-in_rods_and_design_rule_proposal_for_implementation_in_European_standards

Stora Enso. (2017). *Technical brochure*. Retrieved 3.11.2019 from https://www.clt.info/wp-content/uploads/2017/09/CLT-by-Stora-Enso-Technical-manual-EN.pdf

Stora Enso. (2016). *CLT-Cross Laminated Timber. Fire protection*. Retrieved 3.11.2019 from https://www.clt.info/wp-content/uploads/2015/10/CLT-Documentation-on-fire-protection-EN.pdf

Tlustochowicz, G. (2011). *Stabilising System for Multi-Storey Beam and Post Timber Buildings*. Retrieved 12.11.2019 from https://www.diva-portal.org/smash/get/diva2:990624/FULLTEXT01.pdf

Uibel, T. & Blass, H.J. (2007). *Edge joints with dowel type fasteners in cross laminated timber.* Retrieved 9.10.2019 from http://holz.vaka.kit.edu/public/52.pdf